

INT Workshop INT-16-62W

Spectrum and Structure of Excited Nucleons from Exclusive Electroproduction

November 14 - 18, 2016

Nucleon Resonance Spectrum from exclusive meson photo-electroproduction

Annalisa D'Angelo

University of Rome Tor Vergata & INFN Rome Tor Vergata - Rome - Italy

Outline:

- Why study spectroscopy
- Establishing N^* states
- Identifying the effective degrees of freedom
- Outlook & conclusions



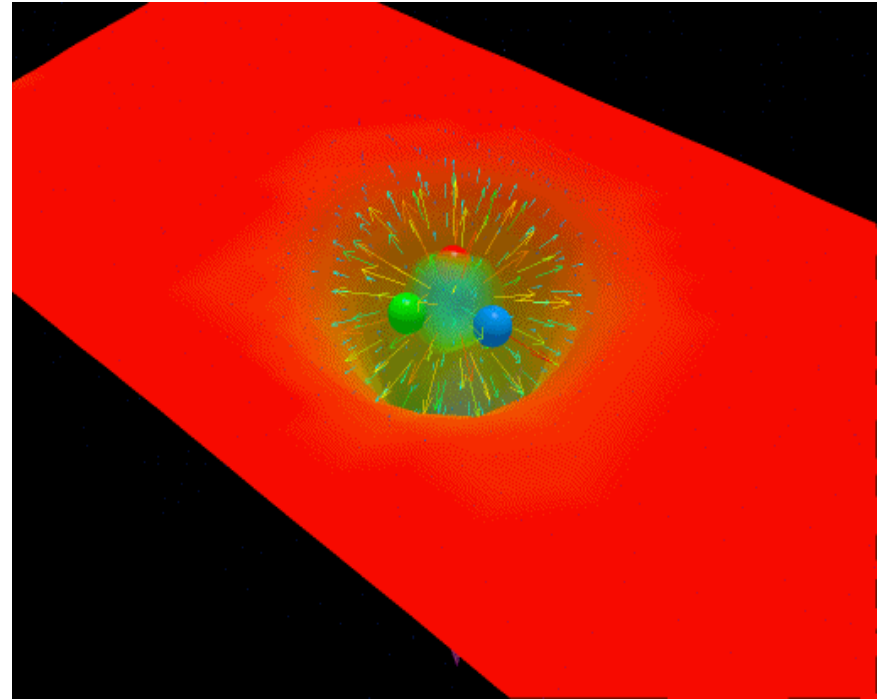
Why N^* ?

Baryon Spectroscopy Reveals the Workings of QCD

“Nucleons are the stuff of which our world is made.

As such they must be at the center of any discussion of why the world we actually experience has the character it does.”

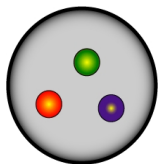
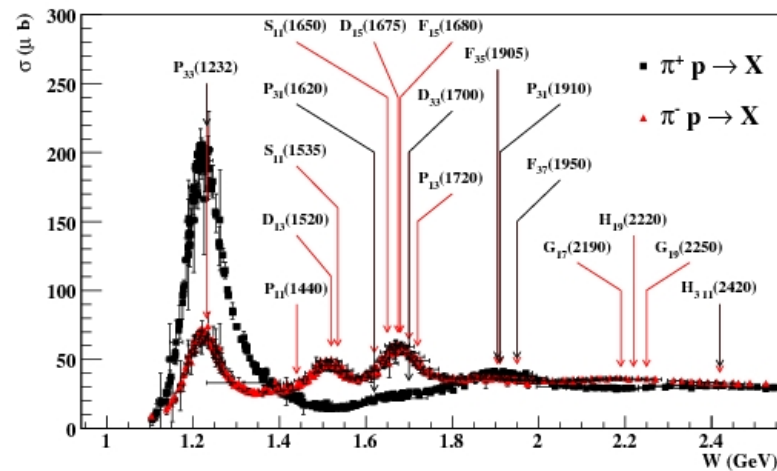
Nathan Isgur, NStar2000, Newport News, Virginia



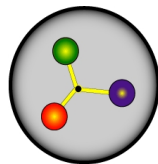
Derek B. Leinweber – University of Adelaide

Why N^* ? From the N^* Spectrum to QCD

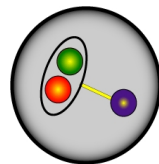
- Understanding the proton's ground state requires understanding its excitation spectrum.
- The N^* spectrum reflects the **effective degrees of freedom** and the forces.



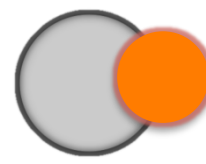
CQM



CQM+flux tubes



Quark-diquark clustering

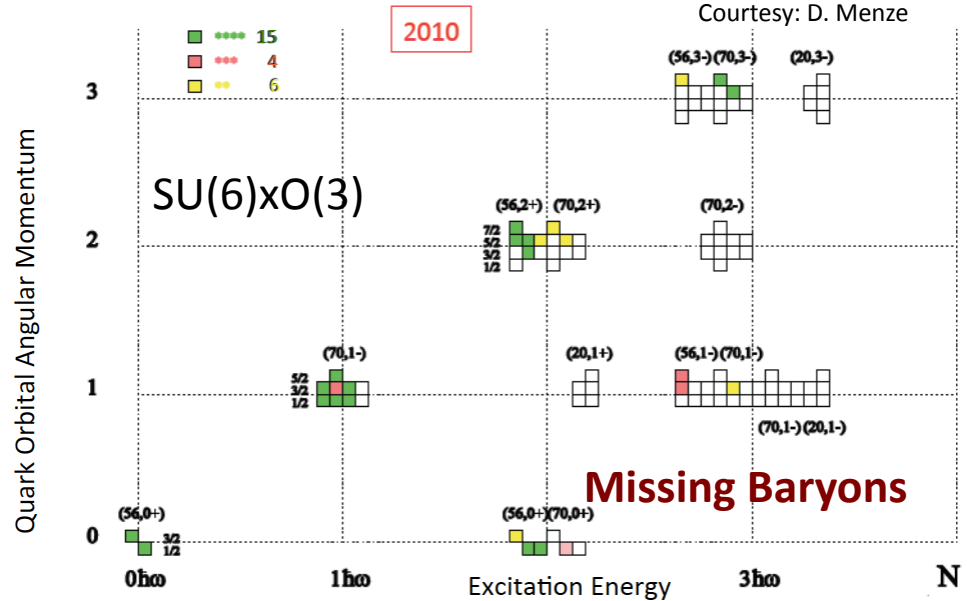
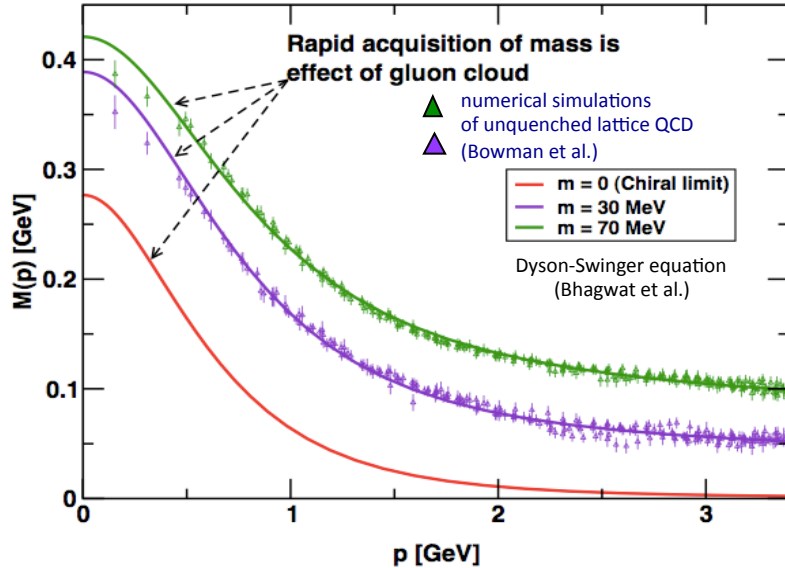


Baryon-meson system



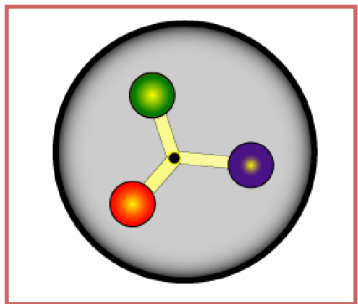
From the Constituent Quark model to QCD.

Constituent quark models and SU(6)xO(3)



- Current-quarks of perturbative QCD evolve into **constituent quarks** at low momentum.
- ➔ **Connection between constituent and current quarks.**
- QCD-inspired Constituent Quark models: states classified by isospin, parity and spin within each oscillator band. **Many projected q^3 states are still missing or uncertain.**

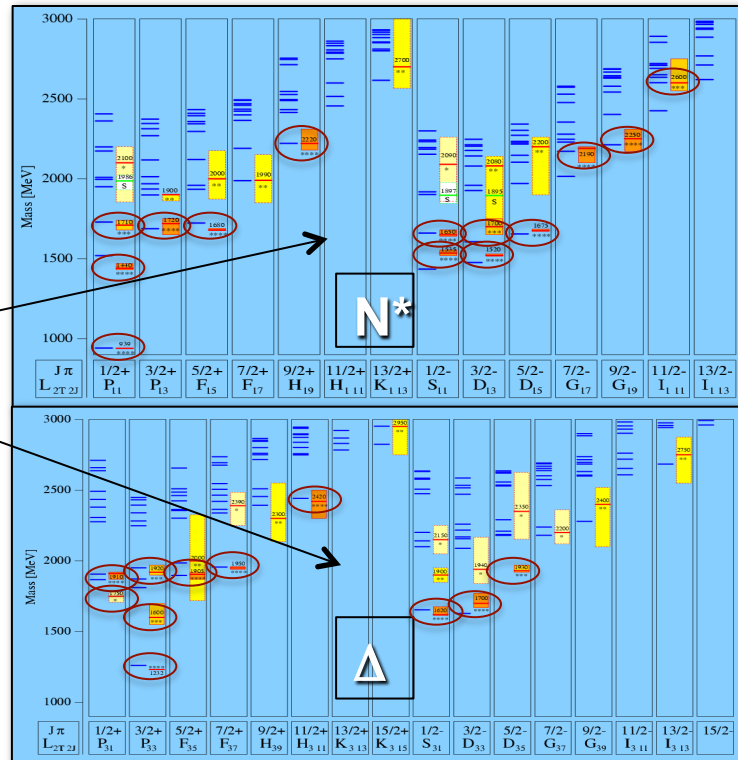
Constituent quark models and SU(6)xO(3)



Thick segments: theoretical predictions
 Shaded boxes: experimental results

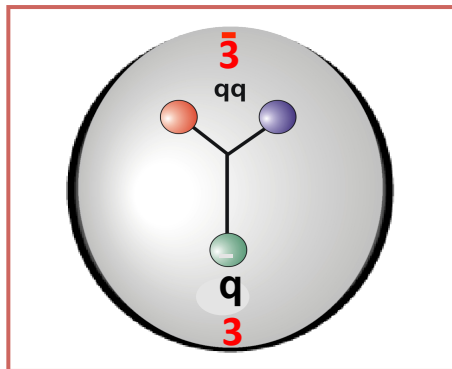
Findings:

- Linear Regge trajectories
- Only lowest few in each band seen with 4★ or 3★ status
- $g(\pi N)$ couplings predicted to decrease rapidly with mass in each oscillator band
- Higher levels predicted to have larger couplings to $K\Lambda$, $K\Sigma$, $\pi\pi N$, ...



U. L'oring, B. Metsch, H. Petry, Eur. Phys. J. A 10, 395 (2001).

QCD-inspired di-Quark Models

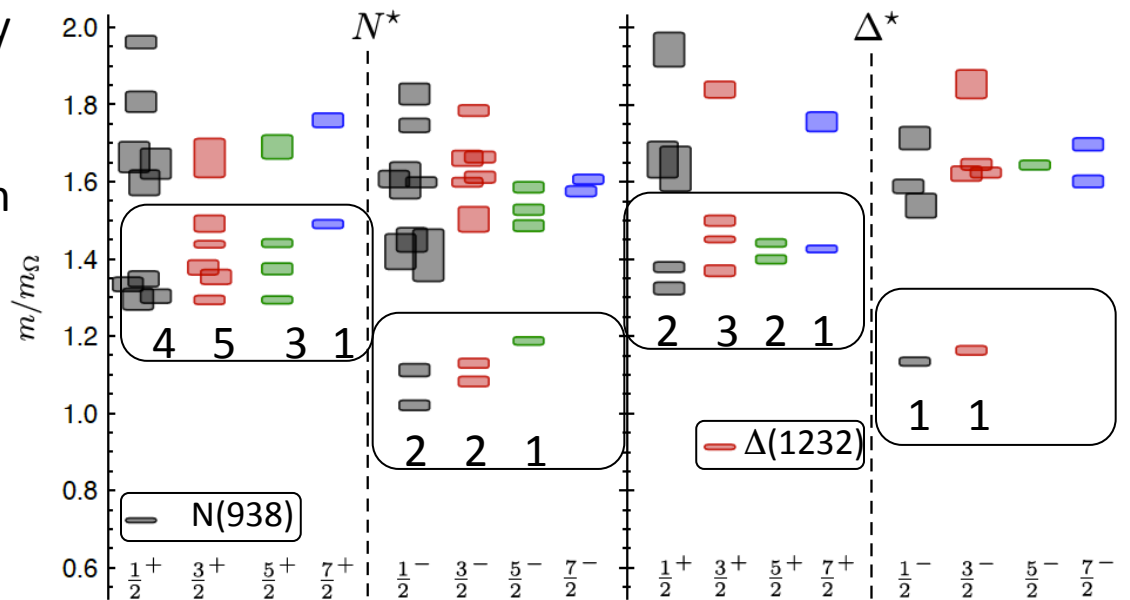


- 2 quarks in nucleon assumed to be quasi-bound in a color isotriplet; diquark-quark is a net color isosinglet.
- All possible internal di-quark excitations \Leftrightarrow full spectrum of CQM.
- Internal di-quark excitations are frozen out (spin 0; isospin 0) \Leftrightarrow large reduction in the number of degrees of freedom \Leftrightarrow may predict less N^* states than seen in πN .

N^*	Status	$SU(6) \otimes U(3)$	Parity	Δ^*	Status	$SU(6) \otimes U(3)$	Parity
$P_{13}(938)$	****	(56, 0 ⁺)	+	$P_{33}(1232)$	****	(56, 0 ⁺)	+
$S_{11}(1535)$	****	(70, 1 ⁻)	-	$S_{31}(1620)$	****	(70, 1 ⁻)	-
$S_{11}(1650)$	****	(70, 1 ⁻)	-	$D_{13}(1700)$	***	(70, 1 ⁻)	-
$D_{13}(1520)$	****	(70, 1 ⁻)	-				
$D_{13}(1700)$	**	(70, 1 ⁻)	-				
$D_{15}(1675)$	****	(70, 1 ⁻)	-				
$P_{11}(1520)$	****	(56, 0 ⁺)	+	$P_{31}(1875)$	****	(56, 2 ⁺)	+
$P_{11}(1710)$	**	(70, 0 ⁺)	+	$P_{31}(1835)$		(70, 0 ⁺)	+
$P_{11}(1880)$		(70, 2 ⁺)	+				
$P_{11}(1975)$		(20, 1 ⁺)	+				
$P_{13}(1720)$	****	(56, 2 ⁺)	+	$P_{33}(1600)$	***	(56, 0 ⁺)	+
$P_{13}(1870)$	*	(70, 0 ⁺)	+	$P_{33}(1920)$	***	(56, 2 ⁺)	+
$P_{13}(1910)$		(70, 2 ⁺)	+	$P_{33}(1985)$		(70, 2 ⁺)	+
$P_{13}(1950)$		(70, 2 ⁺)	+				
$P_{13}(2030)$		(20, 1 ⁺)	+				
$F_{15}(1680)$	****	(56, 2 ⁺)	+	$F_{35}(1905)$	****	(56, 2 ⁺)	+
$F_{15}(2000)$	**	(70, 2 ⁺)	+	$F_{35}(2000)$	**	(70, 2 ⁺)	+
$F_{15}(1995)$		(70, 2 ⁺)	+				
$F_{17}(1990)$	**	(70, 2 ⁺)	+	$F_{37}(1950)$	****	(56, 2 ⁺)	+

LQCD N^* & Δ Spectra

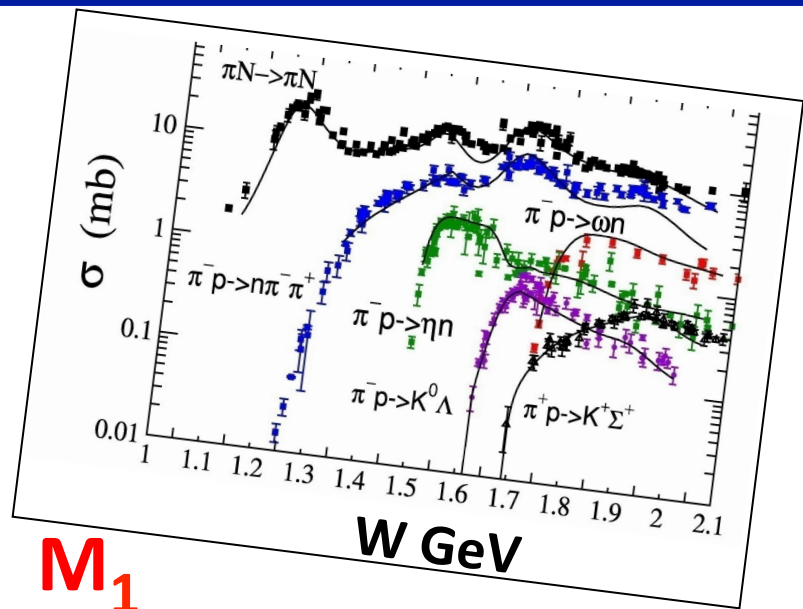
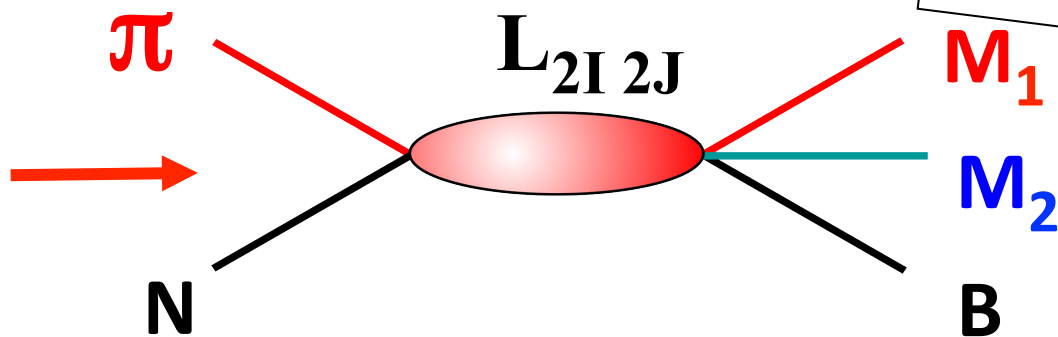
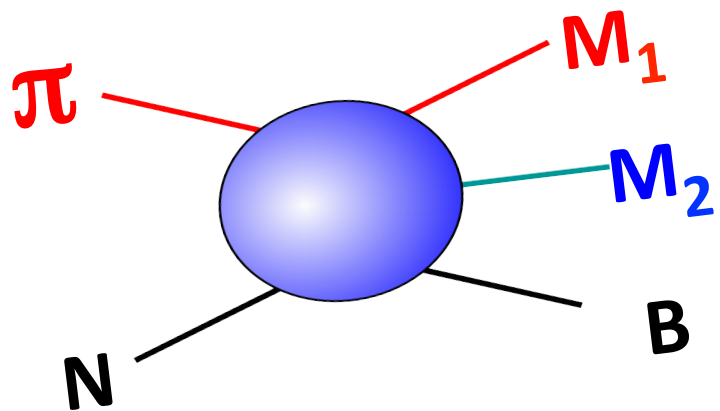
- Exhibit the $SU(6) \times O(3)$ -symmetry features
- Counting of levels consistent with non-rel. quark model
- Striking similarity with quark model
- No parity doubling



Robert G. Edwards, Jozef J. Dudek, David G. Richards, Stephen J. Wallace
 Phys.Rev. D84 (2011) 074508

Problems are not solved!

Establishing the N^* and Δ Spectrum: πN scattering



Establishing the N^* and Δ Spectrum: πN Scattering

$d\sigma/d\Omega$

P Julia-Diaz, Lee, Matsuyama, Sato

$\pi^+ p \rightarrow \pi^+ p$

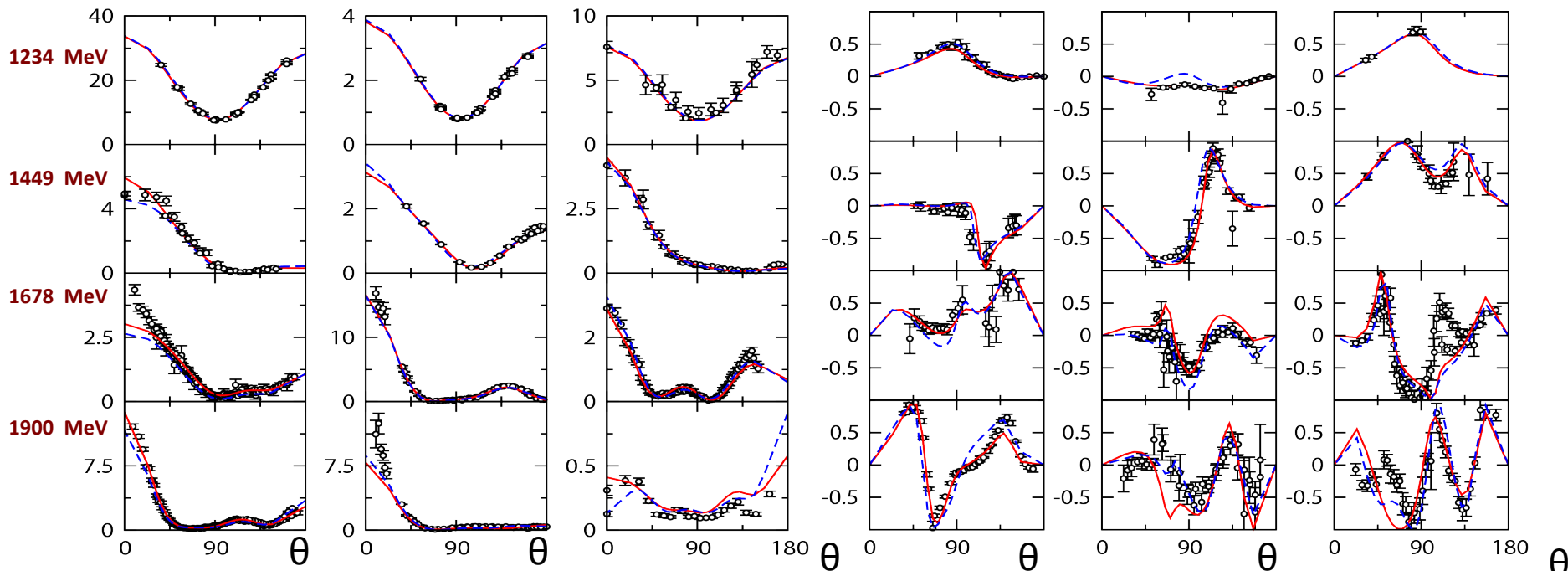
$\pi^- p \rightarrow \pi^- p$

$\pi^- p \rightarrow \pi^0 n$

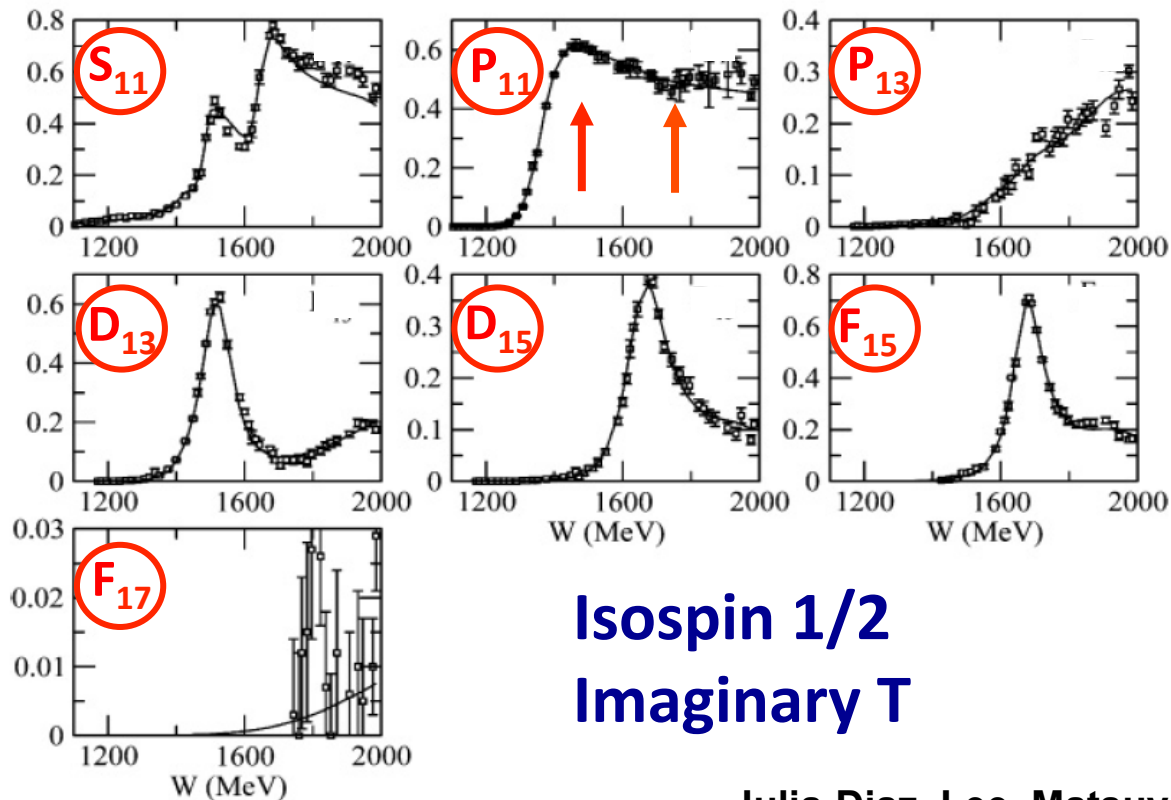
$\pi^+ p \rightarrow \pi^+ p$

$\pi^- p \rightarrow \pi^- p$

$\pi^- p \rightarrow \pi^0 n$



Establishing the N^* and Δ Spectrum: πN Amplitudes

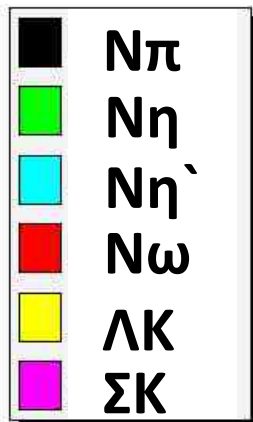
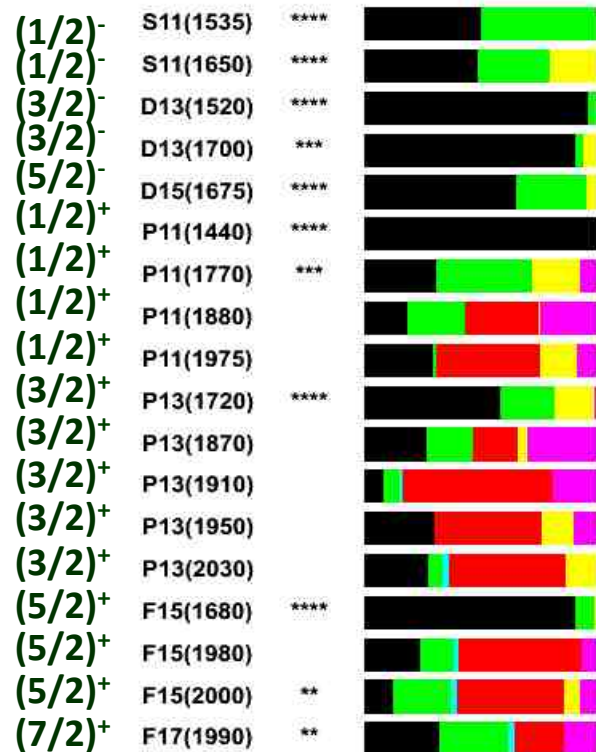


Isospin 1/2
Imaginary T

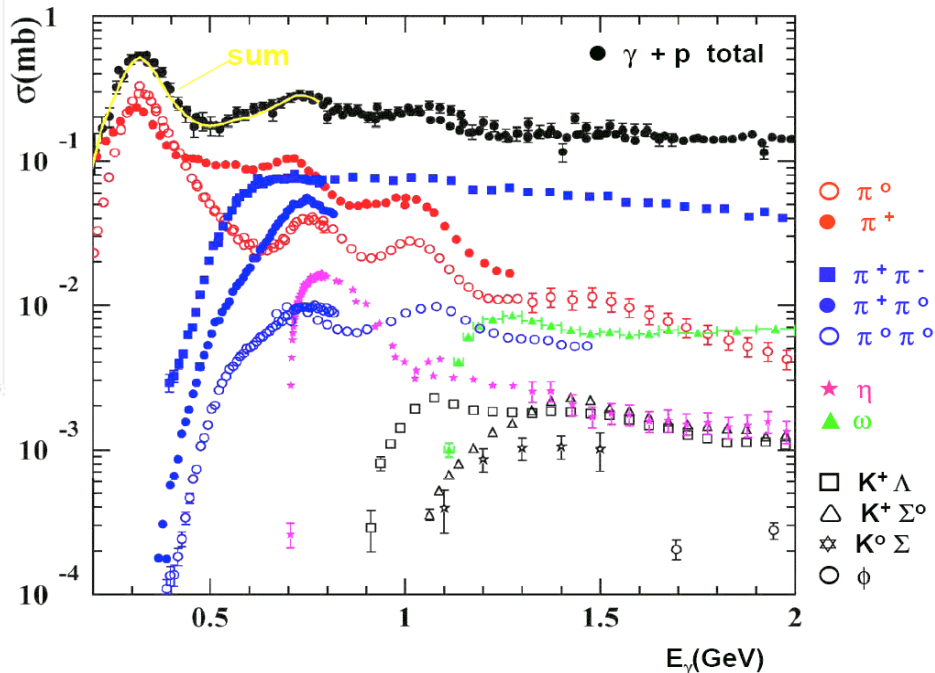
Julia-Diaz, Lee, Matsuyama, Sato

Establishing the N^* and Δ Spectrum

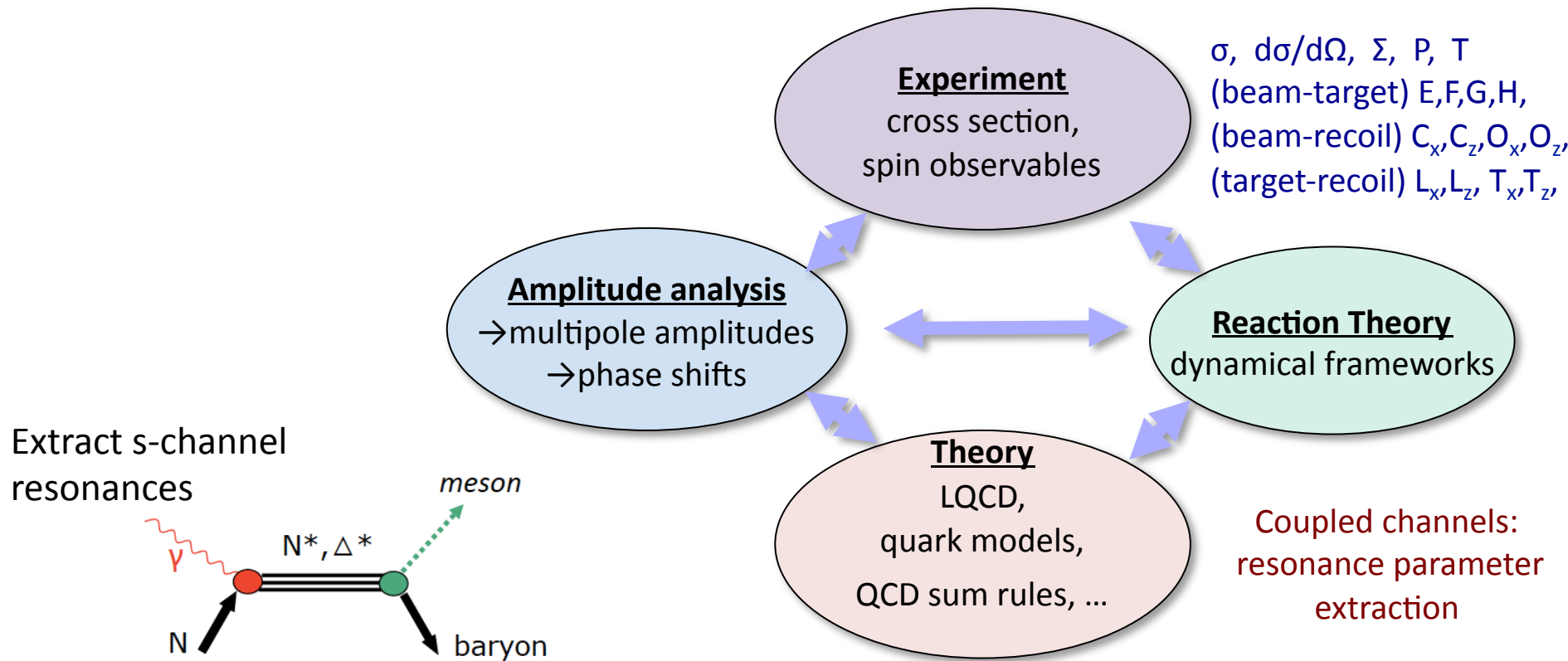
Search all channels: not just πN



Photonuclear cross sections



From Experiment to Theory



From Experiment to Theory

Idealized path to search for N^* , Δ^* states via meson photo-production:

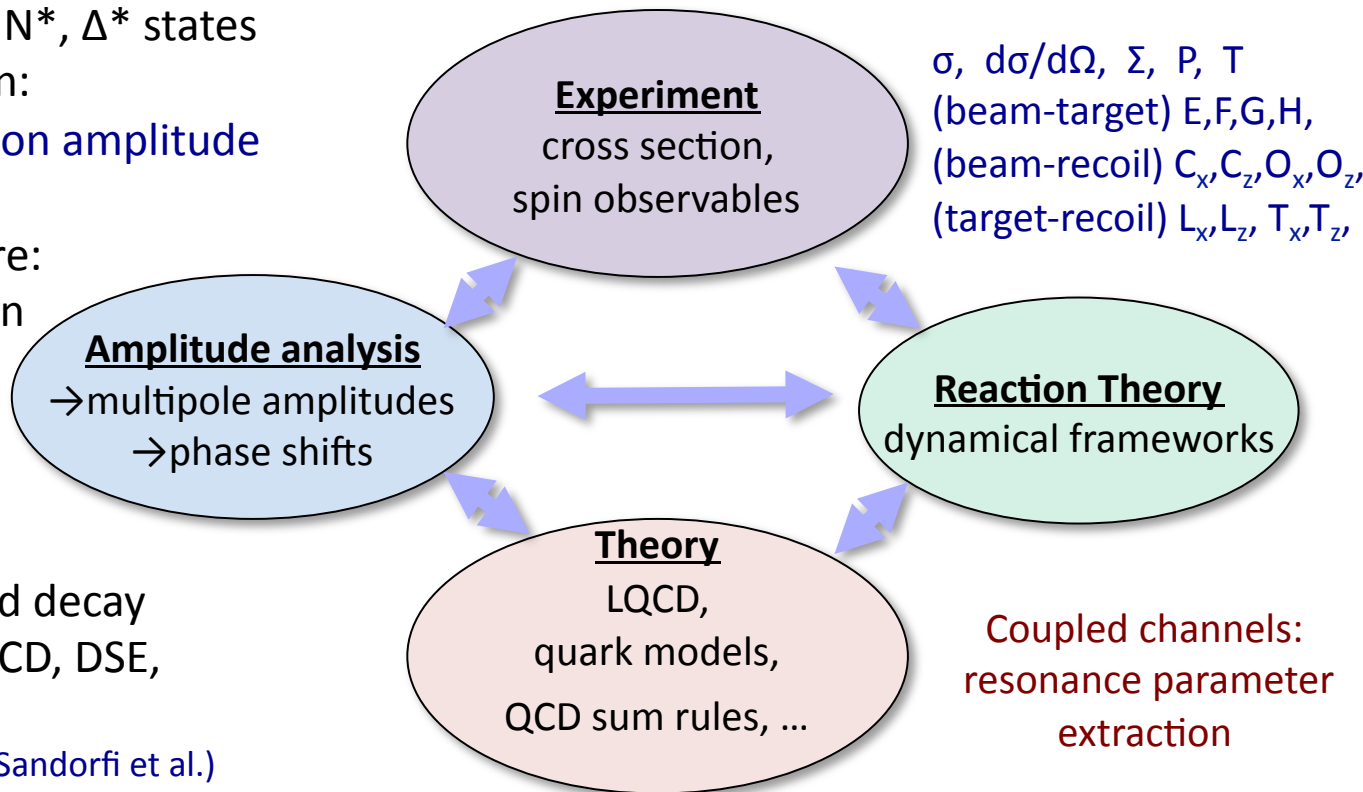
1. determine the production amplitude from experiment

search for resonant structure:
Argand circles, phase motion
speed plots, etc.

2. separate resonance and background components

determine resonant γN^* and decay couplings; contact with LQCD, DSE, Hadron models

(A. Sandorfi et al.)



From Experiment to Theory

Idealized path to search for N^* , Δ^* states
via meson photo-production:

1. determine the production amplitude
from experiment



Never been done after
50 years of experiments

search for resonant structure:
Argand circles, phase motion
speed plots, etc.

2. separate resonance and
background components



Without exp Amplitudes models have
conjectured resonances and adjusted
couplings to compare with limited data

determine resonant γN^* and decay
couplings; contact with LQCD, DSE,
Hadron models

(A. Sandorfi et al.)

Polarization Observables: Complete Experiment

Pseudoscalar Meson Photoproduction

$$\gamma + N \rightarrow m + N$$

$$\begin{array}{cccc} \text{Spin states} & \pm 1 & \pm \frac{1}{2} & 0 & \pm \frac{1}{2} \\ & 2 & \times & 2 & \times & 2 \end{array}$$

8 possible spin states \rightarrow 4 independent complex amplitudes describe the transition matrix

$$F_\lambda = \vec{J} \cdot \hat{\varepsilon}_\lambda = iF_1 \vec{\sigma} \cdot \hat{\varepsilon}_\lambda + F_2 (\hat{\sigma} \cdot \hat{q}) \hat{\sigma} \cdot (\hat{k} \times \hat{\varepsilon}_\lambda) + iF_3 (\hat{\sigma} \cdot \hat{k}) (\hat{q} \cdot \hat{\varepsilon}_\lambda) + iF_4 (\hat{\sigma} \cdot \hat{q}) (\hat{q} \cdot \hat{\varepsilon}_\lambda)$$

CGLN amplitudes in terms
of Pauli matrixes:
are conveniently expanded
into multipoles \longrightarrow

$$F_1 = \sum_{l=0}^{l_{max}} [P'_{l+1}(x)E_{l+} + P'_{l-1}(x)E_{l-} + lP'_{l+1}(x)M_{l+} + (l+1)P'_{l-1}(x)M_{l-}]$$

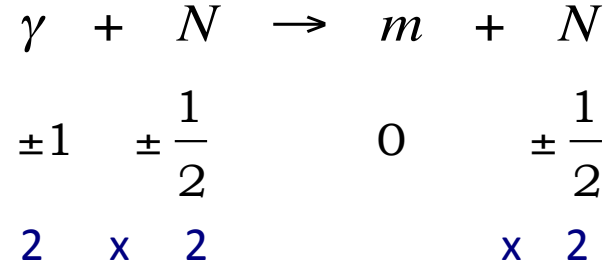
$$F_2 = \sum_{l=0}^{l_{max}} [(l+1)P'_l(x)M_{l+} + lP'_l(x)M_{l-}],$$

$$F_3 = \sum_{l=0}^{l_{max}} [P''_{l+1}(x)E_{l+} + P''_{l-1}(x)E_{l-} - P''_{l+1}(x)M_{l+} + P''_{l-1}(x)M_{l-}],$$

$$F_4 = \sum_{l=0}^{l_{max}} [-P''_l(x)E_{l+} - P''_l(x)E_{l-} + P''_l(x)M_{l+} - P''_l(x)M_{l-}].$$

Polarization Observables: Complete Experiment

Pseudoscalar Meson Photoproduction



Spin states

8 possible spin states \rightarrow 4 independent complex amplitudes describe the transition matrix

Helicity amplitudes: amplitudes are expressed in terms of all independent photon and nucleons helicity states

$$H_1(\theta) \equiv \langle +1 | J_{11} | -1 \rangle$$

$$H_2(\theta) \equiv \langle +1 | J_{11} | +1 \rangle$$

$$H_3(\theta) \equiv \langle -1 | J_{11} | -1 \rangle$$

$$H_4(\theta) \equiv \langle -1 | J_{11} | +1 \rangle$$



$$\begin{aligned} H_1(\theta) &\equiv \frac{i}{\sqrt{2}} \sin\theta \sin\left(\frac{\theta}{2}\right) [F_3 - F_4] \\ H_2(\theta) &\equiv -\frac{i}{\sqrt{2}} \sin\left(\frac{\theta}{2}\right) \left[F_1 + F_2 + (F_4 + F_3) \cos^2\left(\frac{\theta}{2}\right) \right] \\ H_3(\theta) &\equiv +\frac{i}{\sqrt{2}} \sin\theta \cos\left(\frac{\theta}{2}\right) [F_3 + F_4] \\ H_4(\theta) &\equiv -i\sqrt{2} \cos\left(\frac{\theta}{2}\right) \left[F_1 - F_2 + (F_4 - F_3) \sin^2\left(\frac{\theta}{2}\right) \right] \end{aligned}$$

Polarization Observables: Complete Experiment

Pseudoscalar Meson Photoproduction

$$\begin{array}{cccc}
 \gamma & + & N & \rightarrow & m & + & N \\
 \pm 1 & & \pm \frac{1}{2} & & 0 & & \pm \frac{1}{2} \\
 2 & \times & 2 & & & \times & 2
 \end{array}$$

8 possible spin states \rightarrow 4 independent complex amplitudes describe the transition matrix

Helicity amplitudes: amplitudes are expressed in terms of all independent photon and nucleons helicity states

$$H_1(\theta) = \sum_J (2J+1) H_1^J d_{-\frac{1}{2}\frac{3}{2}}^J(\theta),$$

$$H_2(\theta) = \sum_J (2J+1) H_2^J d_{-\frac{1}{2}\frac{1}{2}}^J(\theta),$$

$$H_3(\theta) = \sum_J (2J+1) H_3^J d_{\frac{1}{2}\frac{3}{2}}^J(\theta),$$

$$H_4(\theta) = \sum_J (2J+1) H_4^J d_{\frac{1}{2}\frac{1}{2}}^J(\theta).$$

From decomposition into partial waves:

$$d_{\Lambda_f - \Lambda_i}^J(\theta) \quad \Lambda_i = \lambda - \lambda_1 \quad \Lambda_f = -\lambda_2$$

$$H_4 = N$$

$$H_2, H_3 = S_1, S_2$$

$$H_1 = D$$

no helicity flip

single helicity flip

double helicity flip

Pseudoscalar Meson Photoproduction: Complete Experiment

Transversity amplitudes: are expressed in terms of linearly polarized photons and transversely polarized nucleons. They are linear combinations of helicity amplitudes.

	}	$b_1 = 1/2[(S_1 + S_2) + i(N - D)]$
	}	$b_2 = 1/2[(S_1 + S_2) - i(N - D)]$
	}	$b_3 = 1/2[(S_1 - S_2) - i(N + D)]$
	}	$b_4 = 1/2[(S_1 - S_2) + i(N + D)]$

Pseudoscalar Meson Photoproduction: Complete Experiment

4 complex amplitudes



16 bilinear combinations



16 observables

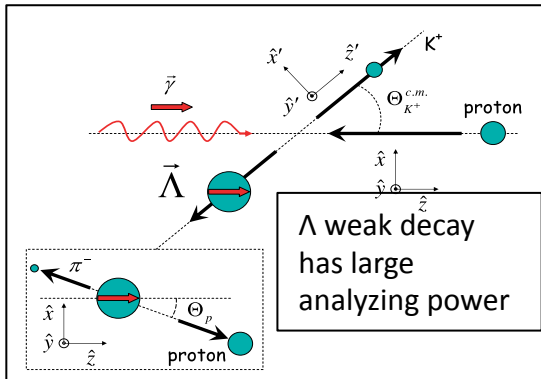
Complete experiment:

at least 8 carefully chosen observables are needed to extract the amplitudes

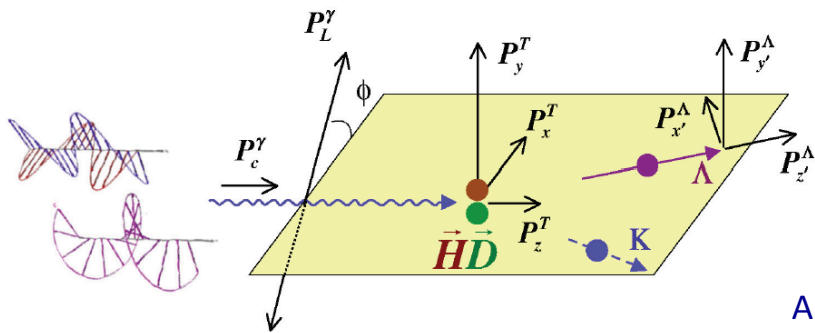
Symbol	Transversity representation	Experiment required	Type
$d\sigma/dt$	$ b_1 ^2 + b_2 ^2 + b_3 ^2 + b_4 ^2$	$\{-; -; -\}$	<i>S</i>
$\Sigma d\sigma/dt$	$ b_1 ^2 + b_2 ^2 - b_3 ^2 - b_4 ^2$	$\{L(\frac{1}{2}\pi, 0); -; -\}$	
$Td\sigma/dt$	$ b_1 ^2 - b_2 ^2 - b_3 ^2 + b_4 ^2$	$\{-; y; -\}$	
$Pd\sigma/dt$	$ b_1 ^2 - b_2 ^2 + b_3 ^2 - b_4 ^2$	$\{-; -; y\}$	
$Gd\sigma/dt$	$2 \operatorname{Im}(b_1 b_3^* + b_2 b_4^*)$	$\{L(\pm\frac{1}{4}\pi); z; -\}$	<i>BT</i>
$Hd\sigma/dt$	$-2 \operatorname{Re}(b_1 b_3^* - b_2 b_4^*)$	$\{L(\pm\frac{1}{4}\pi); x; -\}$	
$Ed\sigma/dt$	$-2 \operatorname{Re}(b_1 b_3^* + b_2 b_4^*)$	$\{C; z; -\}$	
$Fd\sigma/dt$	$2 \operatorname{Im}(b_1 b_3^* - b_2 b_4^*)$	$\{C; x; -\}$	
$O_x d\sigma/dt$	$-2 \operatorname{Re}(b_1 b_4^* - b_2 b_3^*)$	$\{L(\pm\frac{1}{4}\pi); -; x'\}$	<i>BR</i>
$O_z d\sigma/dt$	$-2 \operatorname{Im}(b_1 b_4^* + b_2 b_3^*)$	$\{L(\pm\frac{1}{4}\pi); -; z'\}$	
$C_x d\sigma/dt$	$2 \operatorname{Im}(b_1 b_4^* - b_2 b_3^*)$	$\{C; -; x'\}$	
$C_z d\sigma/dt$	$-2 \operatorname{Re}(b_1 b_4^* + b_2 b_3^*)$	$\{C; -; z'\}$	
$T_x d\sigma/dt$	$2 \operatorname{Re}(b_1 b_2^* - b_3 b_4^*)$	$\{-; x; x'\}$	<i>TR</i>
$T_z d\sigma/dt$	$2 \operatorname{Im}(b_1 b_2^* - b_3 b_4^*)$	$\{-; x; z'\}$	
$L_x d\sigma/dt$	$2 \operatorname{Im}(b_1 b_2^* + b_3 b_4^*)$	$\{-; z; x'\}$	
$L_z d\sigma/dt$	$2 \operatorname{Re}(b_1 b_2^* + b_3 b_4^*)$	$\{-; z; z'\}$	

I. S. Barker, A. Donnachie, J. K. Storrow, Nucl. Phys. B95, 347 (1975).

Pseudoscalar Meson Photoproduction: Complete Experiment



Photon beam	Target			Recoil			Target - Recoil								
				x'	y'	z'	x'	x'	x'	y'	y'	y'	z'	z'	z'
	x	y	z				x	y	z	x	y	z	x	y	z
unpolarized	σ_0	T			P		$T_{x'}$		$L_{x'}$		Σ		$T_{z'}$		$L_{z'}$
$P_L^y \sin(2\phi_\gamma)$		H		G	$O_{x'}$	$O_{z'}$		$C_{z'}$		E		F		$-C_{x'}$	
$P_L^y \cos(2\phi_\gamma)$	$-\Sigma$		$-P$		$-T$		$-L_{z'}$		$T_{z'}$		$-\sigma_0$		$L_{x'}$		$-T_{x'}$
circular P_c^y		F		$-E$	$C_{x'}$	$C_{z'}$		$-O_{z'}$		G		$-H$		$O_{x'}$	



16 different observables, each appearing twice:

- Single-pol observables can be measured from double-pol asymmetry
- Double-pol observables can be measured from triple-pol asymmetry

A. Sandorfi, S. Hoblit, H. Kamano, T.-S.H. Lee, J.Phys. 38 (2011) 053001

Pseudoscalar Meson Photoproduction: Isospin dependence

A^0 and A^1 are the components results from coupling of $I=1/2$ with isoscalar and isovector components of the photon.

Their contributions appear in linear combinations that may be disentangled only by measurements on both the **neutron** and the **proton**.

$$\begin{aligned}
 \mathbf{A}_{\gamma n \rightarrow \begin{pmatrix} \pi^0 n \\ K^0 \Sigma^0 \end{pmatrix}} &= \pm \left[\frac{1}{\sqrt{3}} \mathbf{A}_{\begin{pmatrix} \pi N \\ K \Sigma \end{pmatrix}}^{(0)} + \frac{1}{3} \mathbf{A}_{\begin{pmatrix} \pi N \\ K \Sigma \end{pmatrix}}^{(1)} \right]^{(I=1/2)} + \frac{2}{3} \mathbf{A}_{\begin{pmatrix} \pi N \\ K \Sigma \end{pmatrix}}^{(I=3/2)} \\
 \mathbf{A}_{\gamma n \rightarrow \begin{pmatrix} \pi^- p \\ K^+ \Sigma^- \end{pmatrix}} &= \mp \sqrt{2} \left[\frac{1}{\sqrt{3}} \mathbf{A}_{\begin{pmatrix} \pi N \\ K \Sigma \end{pmatrix}}^{(0)} + \frac{1}{3} \mathbf{A}_{\begin{pmatrix} \pi N \\ K \Sigma \end{pmatrix}}^{(1)} \right]^{(I=1/2)} + \frac{\sqrt{2}}{3} \mathbf{A}_{\begin{pmatrix} \pi N \\ K \Sigma \end{pmatrix}}^{(I=3/2)} \\
 \mathbf{A}_{\gamma n \rightarrow \begin{pmatrix} \eta n \\ K^0 \Lambda \end{pmatrix}} &= + \left[\mathbf{A}_{\begin{pmatrix} \eta N \\ K \Lambda \end{pmatrix}}^{(0)} + \frac{1}{\sqrt{3}} \mathbf{A}_{\begin{pmatrix} \eta N \\ K \Lambda \end{pmatrix}}^{(1)} \right]^{(I=1/2)} \\
 \mathbf{A}_{\gamma p \rightarrow \begin{pmatrix} \pi^0 p \\ K^+ \Sigma^0 \end{pmatrix}} &= \mp \left[\frac{1}{\sqrt{3}} \mathbf{A}_{\begin{pmatrix} \pi N \\ K \Sigma \end{pmatrix}}^{(0)} - \frac{1}{3} \mathbf{A}_{\begin{pmatrix} \pi N \\ K \Sigma \end{pmatrix}}^{(1)} \right]^{(I=1/2)} + \frac{2}{3} \mathbf{A}_{\begin{pmatrix} \pi N \\ K \Sigma \end{pmatrix}}^{(I=3/2)} \\
 \mathbf{A}_{\gamma p \rightarrow \begin{pmatrix} \pi^+ n \\ K^0 \Sigma^+ \end{pmatrix}} &= \pm \sqrt{2} \left[\frac{1}{\sqrt{3}} \mathbf{A}_{\begin{pmatrix} \pi N \\ K \Sigma \end{pmatrix}}^{(0)} - \frac{1}{3} \mathbf{A}_{\begin{pmatrix} \pi N \\ K \Sigma \end{pmatrix}}^{(1)} \right]^{(I=1/2)} + \frac{\sqrt{2}}{3} \mathbf{A}_{\begin{pmatrix} \pi N \\ K \Sigma \end{pmatrix}}^{(I=3/2)} \\
 \mathbf{A}_{\gamma p \rightarrow \begin{pmatrix} \eta p \\ K^+ \Lambda \end{pmatrix}} &= + \left[\mathbf{A}_{\begin{pmatrix} \eta N \\ K \Lambda \end{pmatrix}}^{(0)} - \frac{1}{\sqrt{3}} \mathbf{A}_{\begin{pmatrix} \eta N \\ K \Lambda \end{pmatrix}}^{(1)} \right]^{(I=1/2)}
 \end{aligned}$$

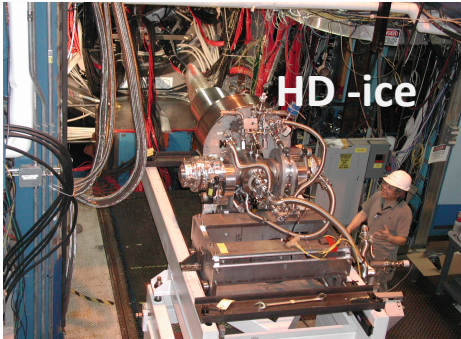
I. S. Barker, A. Donnachie, J. K. Storrow, Nucl. Phys. B95, 347 (1975).

Experimental set-up

Polarized Frozen-spin Targets & CEBAF Large Acceptance Spectrometer



or



+

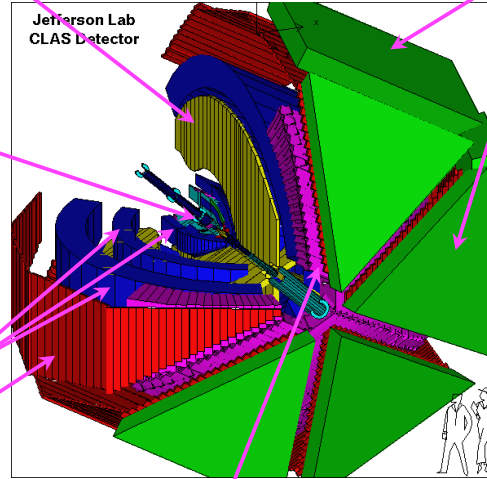
start counter



Drift chambers
35,000 cells

Time-of-flight counters
plastic scintillators,
684 photomultipliers

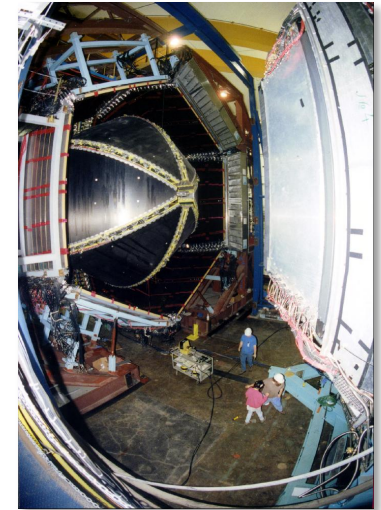
Torus magnet
6 superconducting coils



Gas Cherenkov counters
 e/π separation, 256 PMTs

Electromagnetic calorimeters
Lead/scintillator, 1296 photomultipliers

Open CLAS detector



CLAS N* Experimental Program

	σ	Σ	T	P	E	F	G	H	T_x	T_z	L_x	L_z	O_x	O_z	C_x	C_z
$p\pi^0$	✓	✓	✓		✓	✓	✓	✓								
$n\pi^+$	✓	✓	✓		✓	✓	✓	✓								
$p\eta$	✓	✓	✓		✓	✓	✓	✓								
$p\eta'$	✓	✓	✓		✓	✓	✓	✓								
$p\omega/\phi$	✓	✓	✓		✓	✓	✓	✓								
$N\pi\pi$	✓	✓														
$K^+\Lambda$	✓	✓	✓	✓	✓	✓	✓	✓	✓	✓	✓	✓	✓	✓	✓	✓
$K^+\Sigma^0$	✓	✓	✓	✓	✓	✓	✓	✓	✓	✓	✓	✓	✓	✓	✓	✓
$K^0*\Sigma^+$	✓	✓									✓	✓				
$K^{*0}\Sigma^0$	✓	✓														
$p\pi^-$	✓	✓			✓	✓	✓									
$p\rho^-$	✓	✓			✓	✓	✓									
$K^-\Sigma^+$	✓	✓			✓	✓	✓									
$K^0\Lambda$	✓	✓		✓	✓	✓	✓				✓	✓	✓	✓	✓	✓
$K^0\Sigma^0$	✓	✓		✓	✓	✓	✓				✓	✓	✓	✓	✓	✓
$K^0*\Sigma^0$	✓	✓														

Proton targets

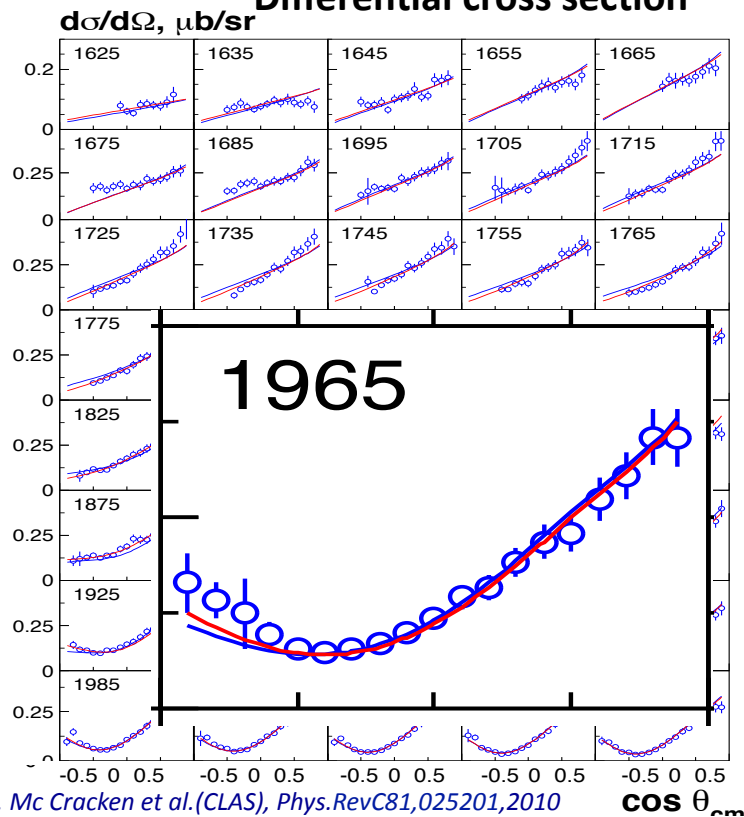
Data taking completed May 18, 2012

✓-published, ✓-acquired

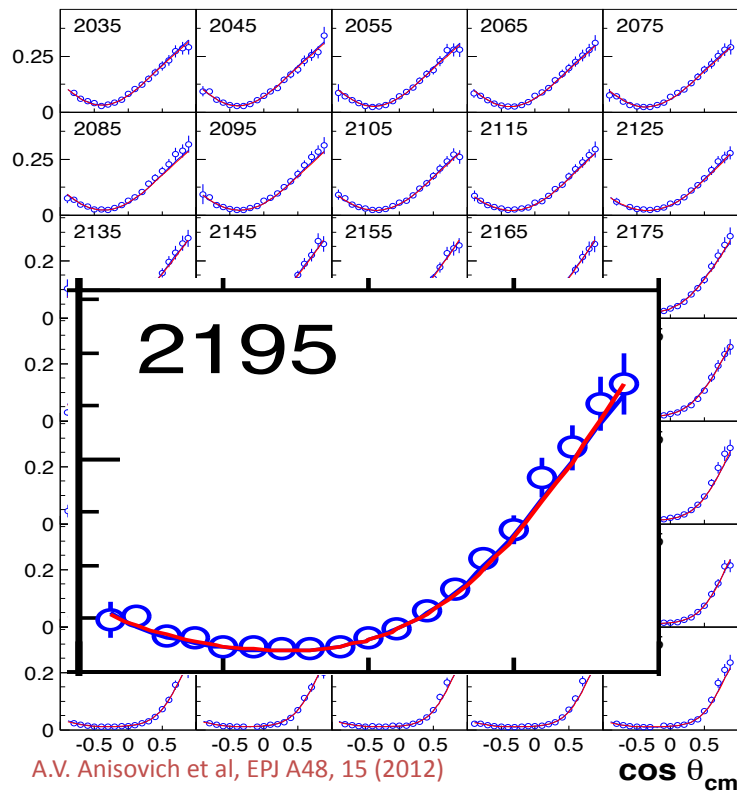
Neutron targets

Strangeness production: $\vec{\gamma} + \vec{p} \rightarrow K^+ + \vec{\Lambda} \rightarrow K^+ + p + \pi^-$

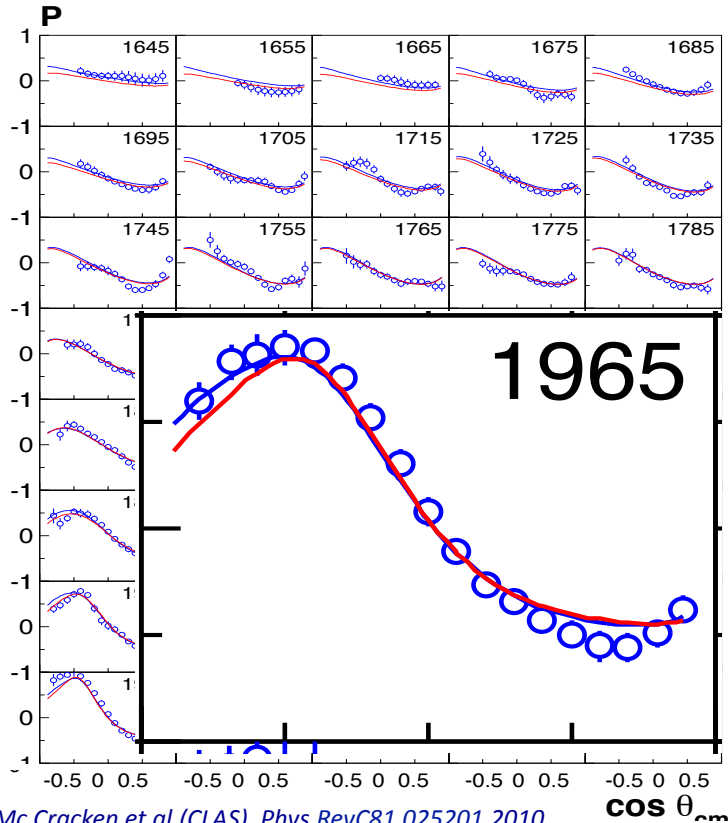
Differential cross section



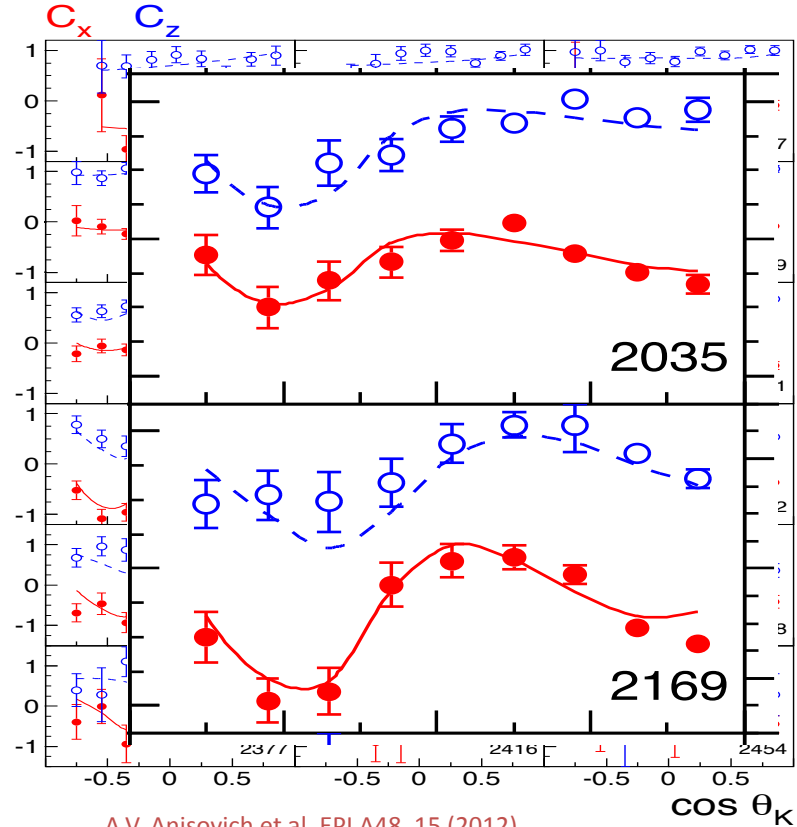
Σ Beam Asymmetry



Strangeness production: $\vec{\gamma} + \vec{p} \rightarrow K^+ + \vec{\Lambda} \rightarrow K^+ + p + \pi^-$



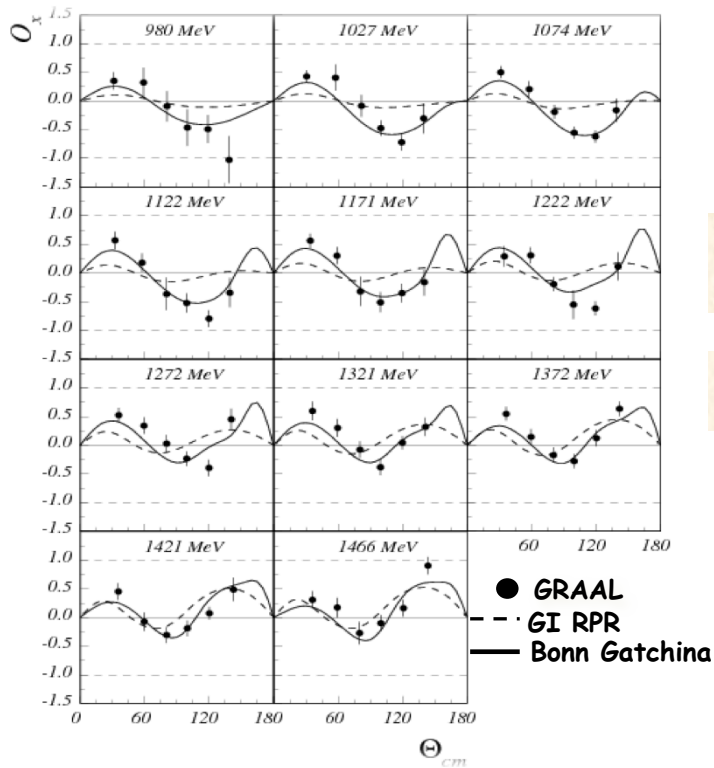
M. Mc Cracken et al. (CLAS), *Phys.RevC81,025201,2010*



A.V. Anisovich et al, *EPJ A48, 15 (2012)*

Strangeness production: $\vec{\gamma} + \vec{p} \rightarrow K^+ + \vec{\Lambda} \rightarrow K^+ + p + \pi^-$

A.Lleres et al., EPJ A 39, 149-161 (2009)

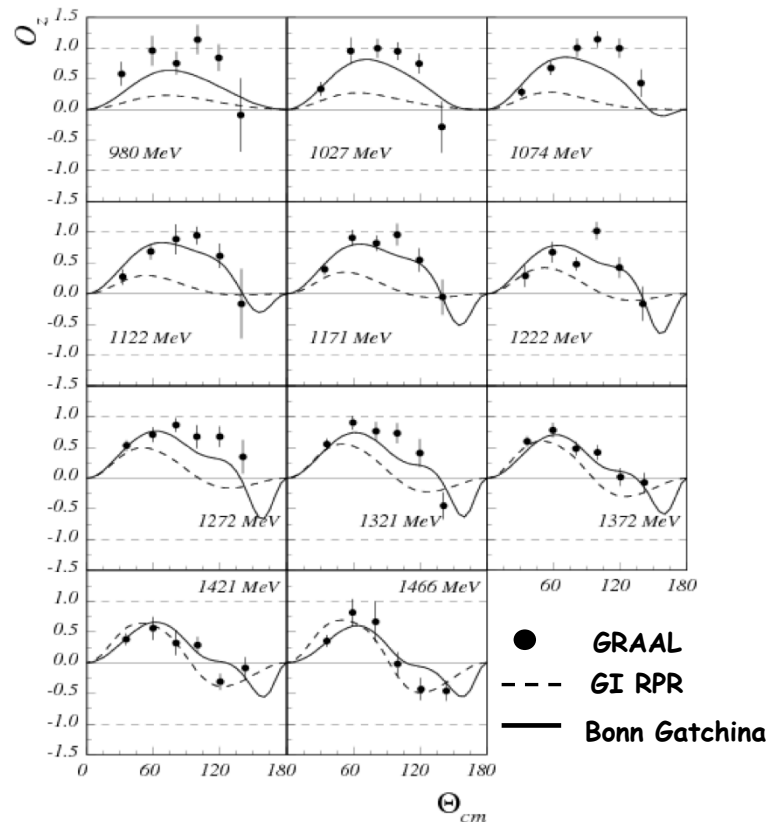


O_x, O_z Double Polarization Asymmetries

$$\frac{2N_+^{x'}}{N_+^{x'} + N_-^{x'}} = \left(1 + \alpha \frac{2P_\gamma O_x}{\pi} \cos\theta_p^{x'} \right)$$

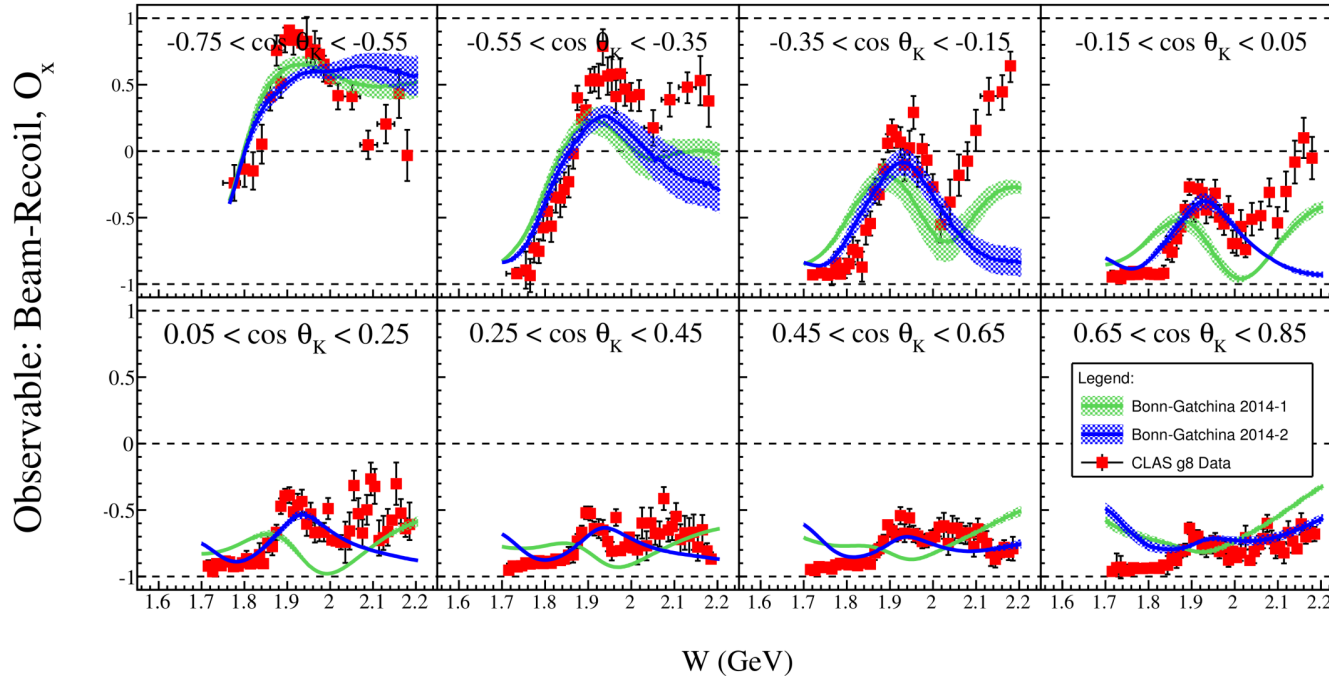
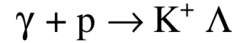
$$\frac{2N_+^{z'}}{N_+^{z'} + N_-^{z'}} = \left(1 + \alpha \frac{2P_\gamma O_z}{\pi} \cos\theta_p^{z'} \right)$$

GRAAL Experiment



Strangeness production: $\vec{\gamma} + \vec{p} \rightarrow K^+ + \vec{\Lambda} \rightarrow K^+ + p + \pi^-$

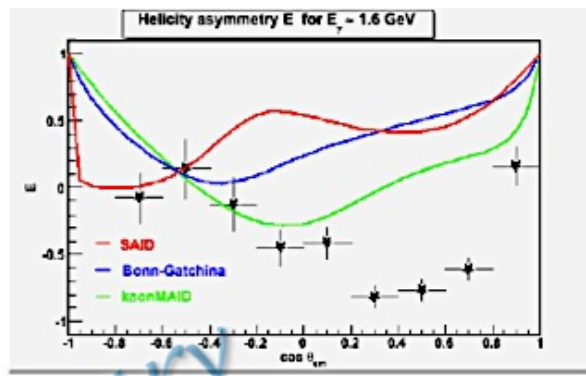
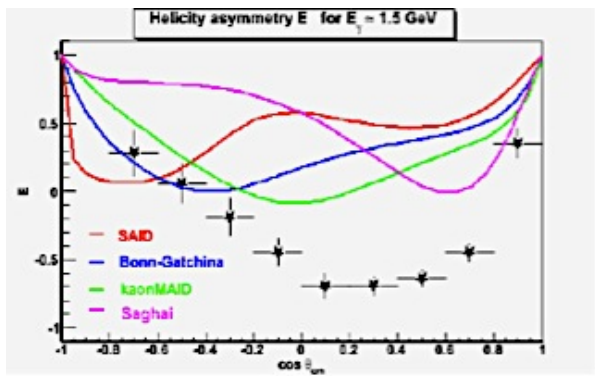
D. Ireland



O_x Double
Polarization
Asymmetry

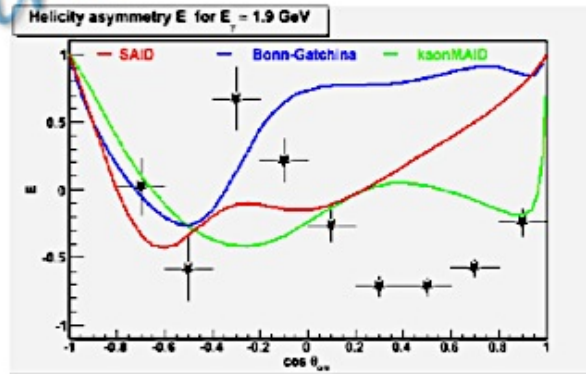
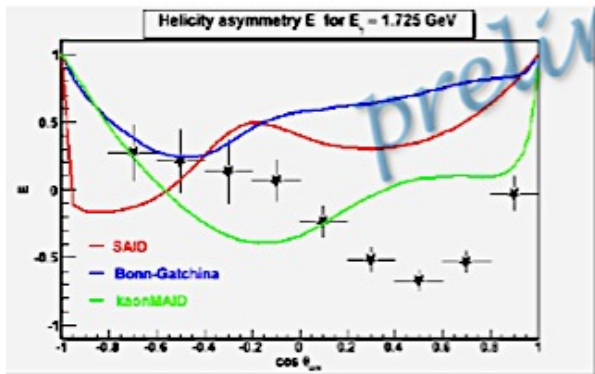
CLAS
Experiment

Strangeness production: $\vec{\gamma} + \vec{p} \rightarrow K^+ + \vec{\Lambda} \rightarrow K^+ + p + \pi^-$



E Polarization
Asymmetry

CLAS
Experiment



L. Casey, Catholic Univ.

Strangeness production: $\vec{\gamma} + \vec{p} \rightarrow K^+ + \vec{\Lambda} \rightarrow K^+ + p + \pi^-$

A.Lleres et al., EPJ A 39, 149-161 (2009)

From $O_{x'}$, O_z and T results:

- Ghent Isobar RPR Model:

$$S_{11}(1650) \quad P_{11}(1710) \quad P_{13}(1720)$$

$$P_{13}(1900) \quad D_{13}(1900)$$

- Bonn Gatchina Model:

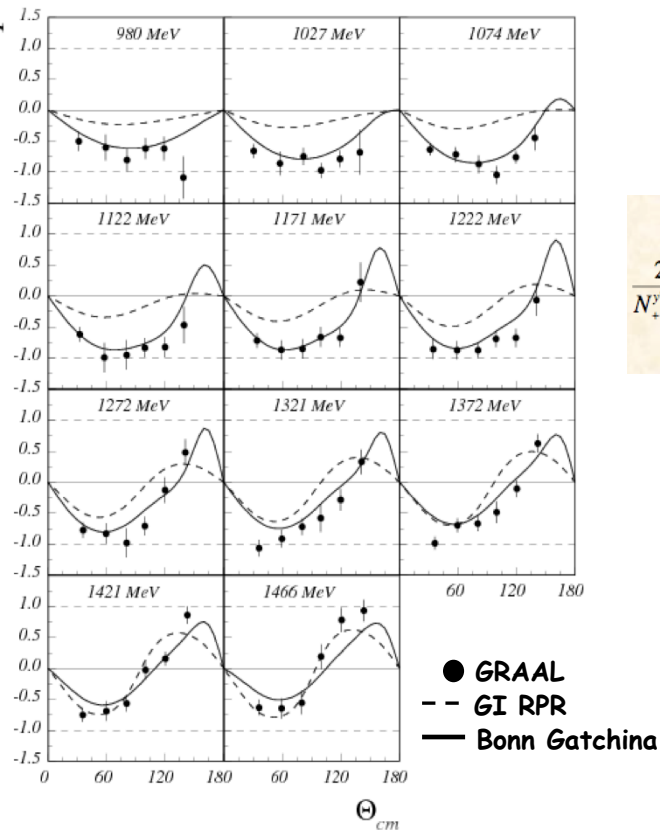
$$S_{11}(1535) \quad S_{11}(1650) \quad P_{11}(1840)$$

$$P_{13}(1900)$$

T asymmetry from P_y and Σ polarization observables

$$\frac{2N_+^{y'}}{N_+^{y'} + N_-^{y'}} = \left(1 + \frac{2P_y \Sigma}{\pi} \right) \left(\frac{1 + \alpha \frac{P\pi + 2P_y T}{\pi + 2P_y \Sigma} \cos \theta_p^{y'}}{1 + \alpha P \cos \theta_p^{y'}} \right)$$

GRAAL
Experiment



Updated Spectrum of Baryon Resonances

- From 2000 to 2010 no new Baryon resonances were considered by the PDG.
 - Used πN - scattering data and some π -photoproduction only.
- Mature multi-channel models now include many photoproduction data.
- E.g. Bonn-Gatchina PWA analysis, A. Anisovich et al. EPJ A 48, 15 (2012).

	Particle Data Group 2010	BnGa analyses	Particle Data Group 2012
N(1860)5/2 ⁺		*	**
N(1875)3/2 ⁻		***	***
N(1880)1/2 ⁺		**	**
N(1895)1/2 ⁻		**	**
N(1900)3/2 ⁺	**	***	***
N(2060)5/2 ⁻		***	**
N(2150)3/2 ⁻		**	**
$\Delta(1940)3/2^-$	*	*	**

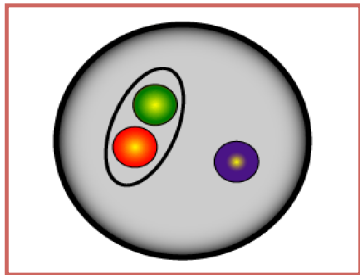
Naming scheme has changed:

$$L_{2I} 2J(E) \longrightarrow J^P(E)$$

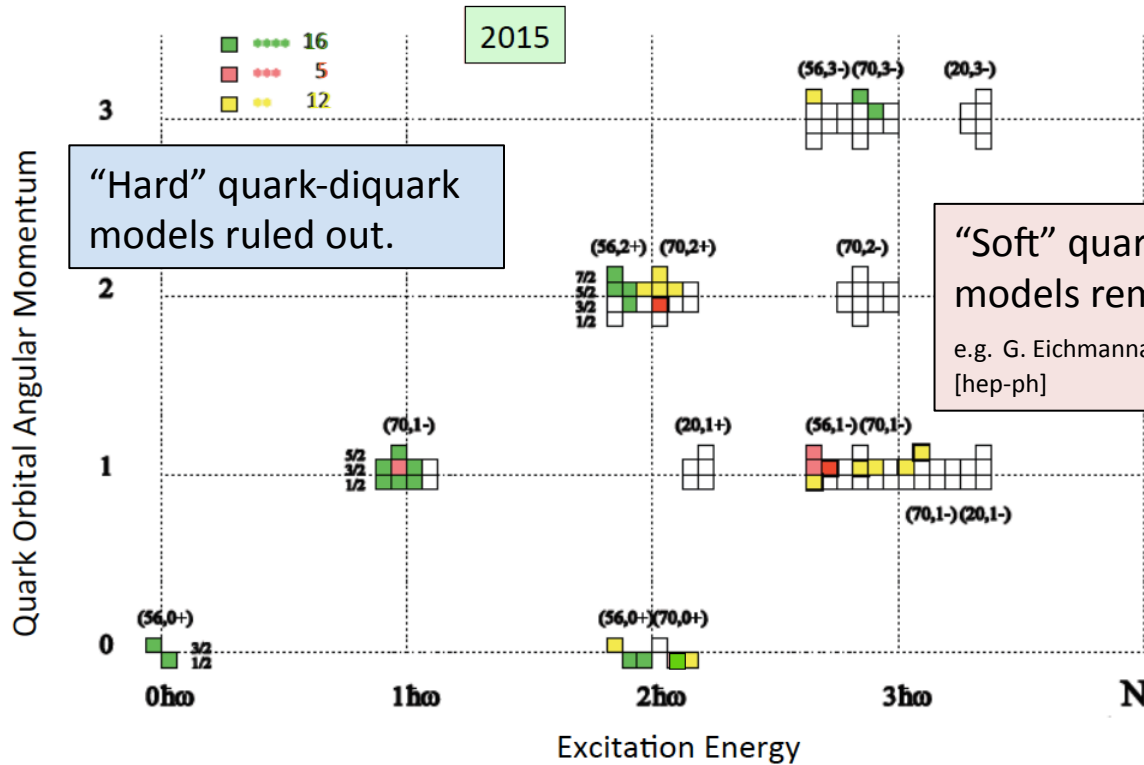
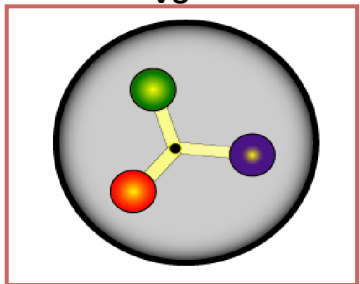
- Results from photoproduction now add to the PDG tables and determine properties of baryon resonances

Do New States Fit into Q^3 QM ?

$SU(6) \times O(3)$



VS



Do New States Fit into LQCD Projections ?

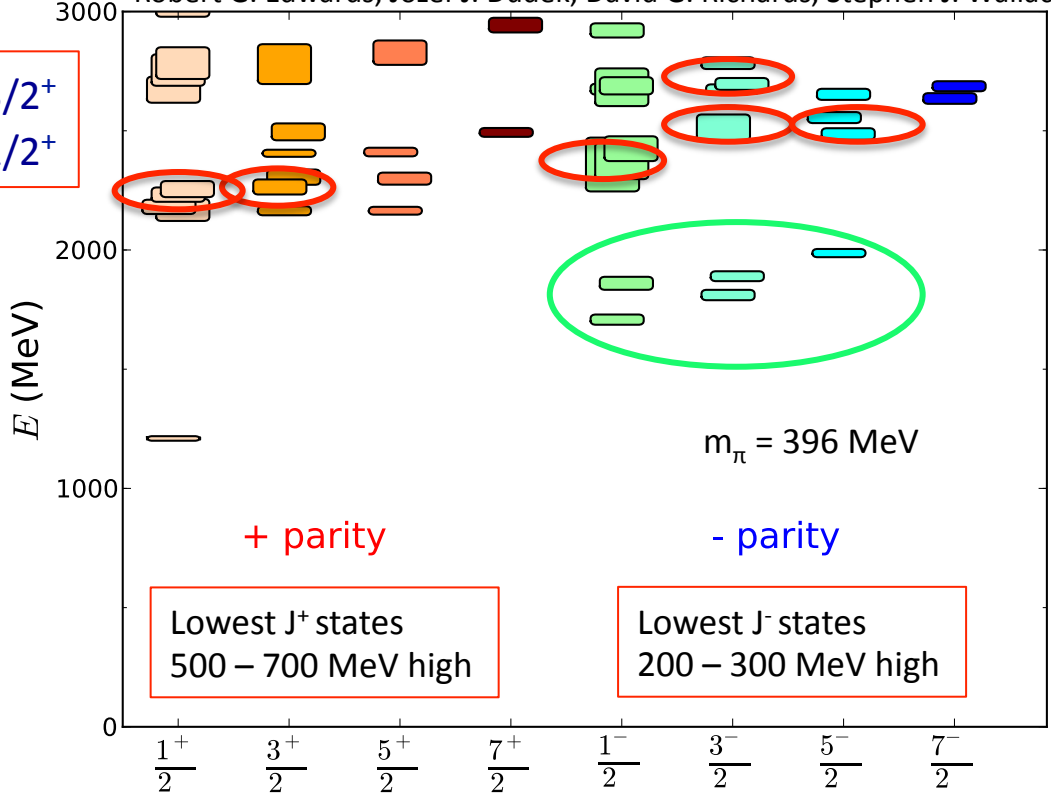
Robert G. Edwards, Jozef J. Dudek, David G. Richards, Stephen J. Wallace *Phys.Rev. D84 (2011) 074508*

$N(1900)3/2^+$
 $N(1880)1/2^+$

$N(2060)5/2^-$
 $N(2120)3/2^-$
 $N(1875)3/2^-$
 $N(1895)1/2^-$

Ignoring the mass scale, new candidates fit the J^P values predicted from LQCD.

The field would really benefit from more realistic Lattice masses for N^* states.



Known states:
 $N(1675)5/2^-$
 $N(1700)3/2^-$
 $N(1520)3/2^-$
 $N(1650)1/2^-$
 $N(1535)1/2^-$

Results on Polarized Neutron Target



On-going Analyses:

- T. Kageya (Jlab): $\gamma_c n(p) \rightarrow \pi^- p(p)$
- H. Lu (CMU, U. Iowa): $\gamma_L n(p) \rightarrow \pi^- p(p)$
- P. Peng (U. Virginia): $\gamma_c p \rightarrow \pi^+ \pi^- p$; $\gamma_c n(p) \rightarrow \pi^+ \pi^- n(p)$
- J. Fleming (U. Edinburgh): $\gamma_L p \rightarrow \pi^+ \pi^- p$; $\gamma_L n(p) \rightarrow \pi^+ \pi^- n(p)$
 $\gamma_c n(p) \rightarrow K^+ \Sigma^-(p)$
- I. Zonta (U. Roma-II): $\gamma_c n(p) \rightarrow \rho n(p) \rightarrow \pi^+ \pi^- n(p)$
- D. Ho (Carnegie-Mellon U.): $\gamma_c n(p) \rightarrow K^0 \Lambda(p)$

⇒ some examples with $\sim \frac{1}{3}$ to $\frac{2}{3}$ data processed

Results on Polarized Neutron Target



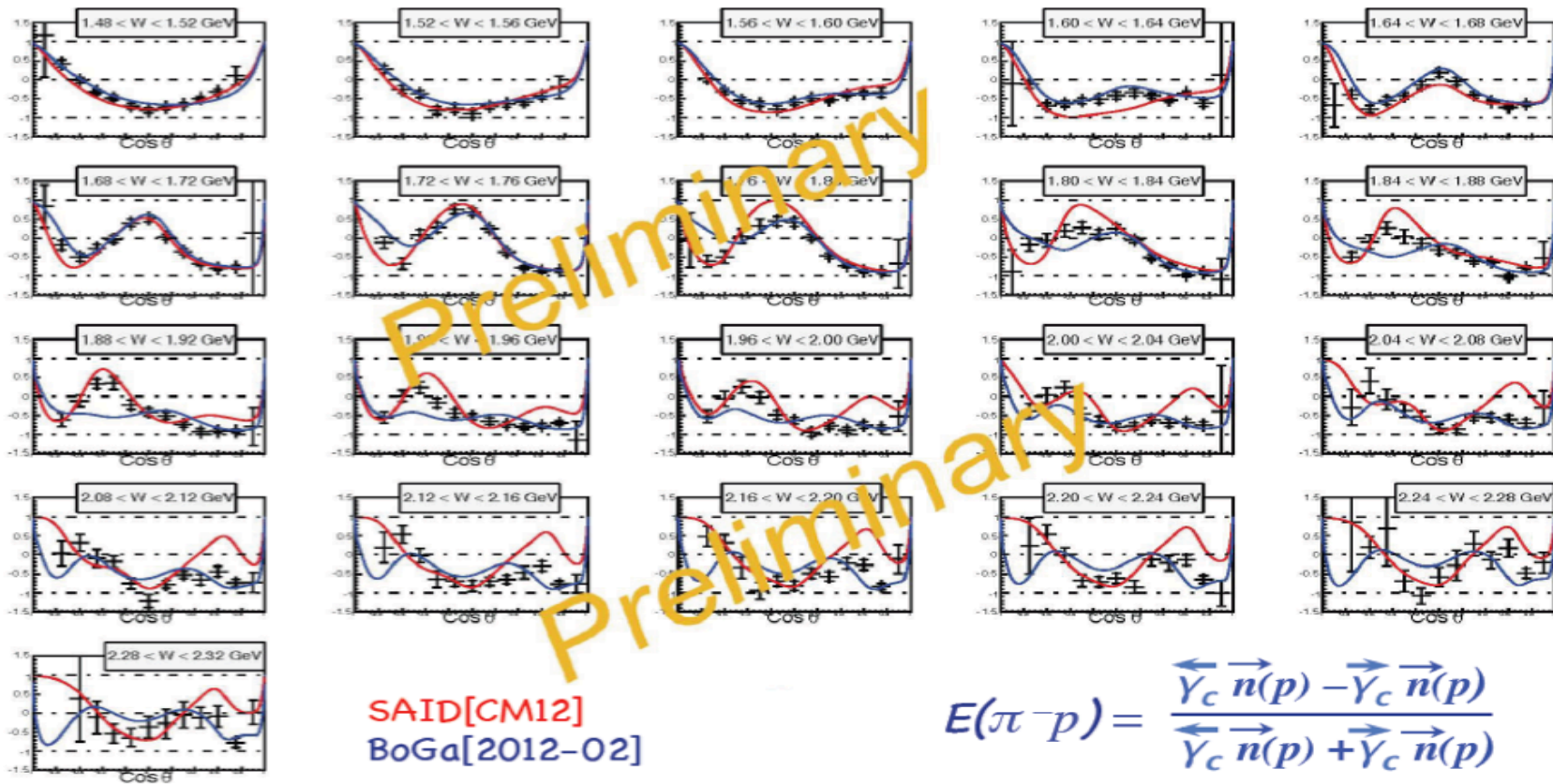
On-going Analyses:

- T. Kageya (Jlab): $\gamma_c n(p) \rightarrow \pi^- p(p)$ Different bkg removal methods
Empty cell
Subtraction
- H. Lu (CMU, U. Iowa): $\gamma_L n(p) \rightarrow \pi^- p(p)$ Kinematical fitting
- P. Peng (U. Virginia): $\gamma_c p \rightarrow \pi^+ \pi^- p; \gamma_c n(p) \rightarrow \pi^+ \pi^- n(p)$
- J. Fleming (U. Edinburgh): $\gamma_L p \rightarrow \pi^+ \pi^- p; \gamma_L n(p) \rightarrow \pi^+ \pi^- n(p)$
 $\gamma_c n(p) \rightarrow K^+ \Sigma^-(p)$
- I. Zonta (U. Roma-II): $\gamma_c n(p) \rightarrow \rho n(p) \rightarrow \pi^+ \pi^- n(p)$ Empty cell
Subtraction
- D. Ho (Carnegie-Mellon U.): $\gamma_c n(p) \rightarrow K^0 \Lambda(p)$ Boosted Decision Trees

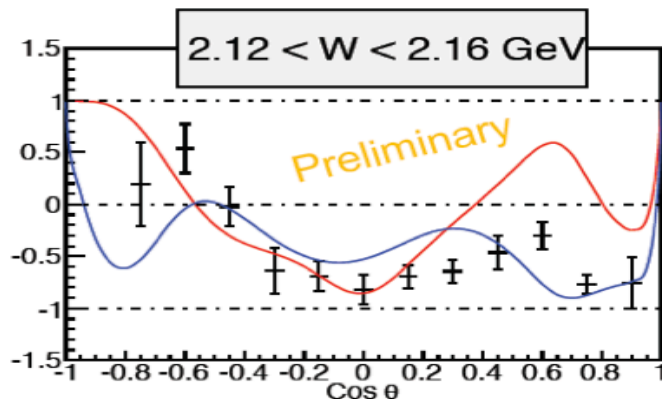
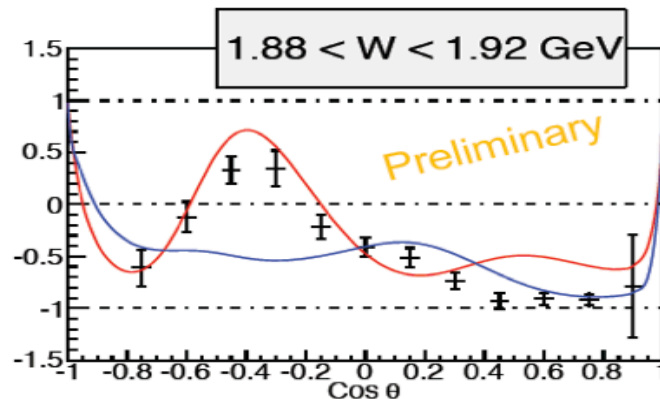
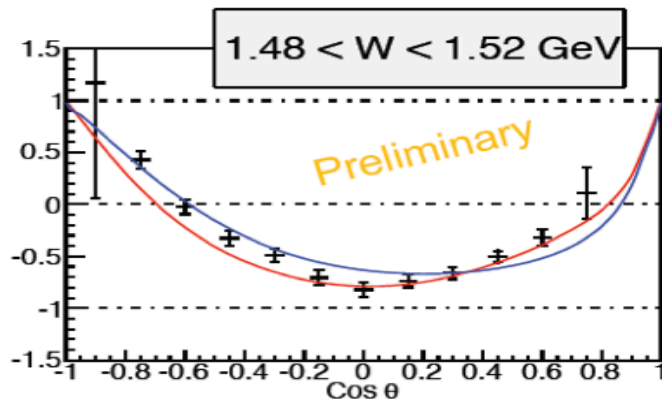
A.M. Sandorfi -

⇒ some examples with $\sim \frac{1}{3}$ to $\frac{2}{3}$ data processed

$\gamma d \rightarrow \pi^- p(p)$ Helicity Asymmetry E



$\gamma d \rightarrow \pi^- p(p)$ Helicity Asymmetry E



$$E(\pi^- p) = \frac{\overleftarrow{\gamma}_c \overrightarrow{n}(p) - \overrightarrow{\gamma}_c \overrightarrow{n}(p)}{\overleftarrow{\gamma}_c \overrightarrow{n}(p) + \overrightarrow{\gamma}_c \overrightarrow{n}(p)}$$

T. Kageya PWA:
A.M. Sandorfi -

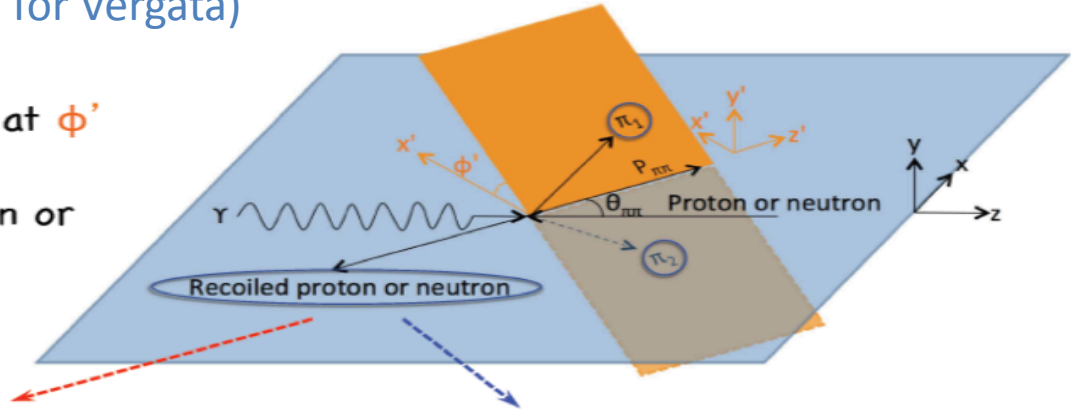
SAID[CM12]
BoGa[2012-02]

$\gamma p \rightarrow \pi^+ \pi^- p$ and $\gamma d \rightarrow \pi^+ \pi^- n(p)$

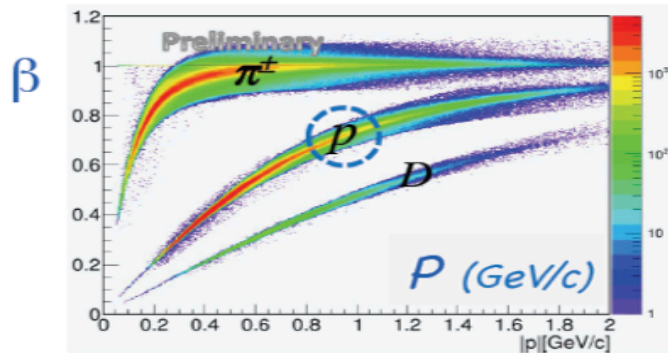


P. Peng (UVA), I. Zonta (U. Roma Tor Vergata)

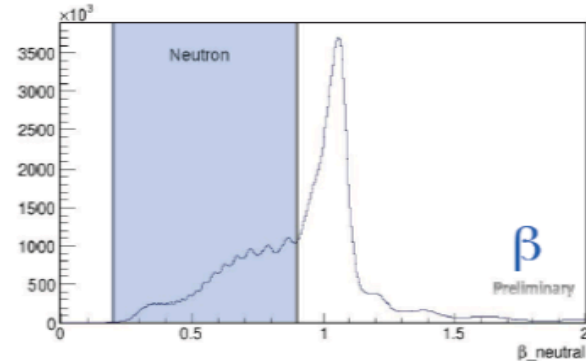
- elementary $d^5\sigma$
- $\pi^+ \pi^-$ define a plane at ϕ' wrt reaction plane
- observables are even or odd wrt ϕ'
- $P_{\pi\pi}(\theta_{\pi\pi}) = P_{\pi^+} + P_{\pi^-}$



protons in drift chambers



neutrons in forward calorimeter



$\gamma p \rightarrow \pi^+ \pi^- p$ and $\gamma d \rightarrow \pi^+ \pi^- n(p)$



- in the notation of Roberts and Oed, PR C71 (05) 055201
- 64 possible **polarization observables**; ≥ 15 needed to determine amplitude

$$\frac{d\sigma^{BT}}{d\Omega} = d\sigma_0 \left\{ \begin{aligned} & \left((1 + \vec{\Lambda} \cdot \vec{P}) + \delta_{\odot} (I^{\odot} + \vec{\Lambda} \cdot \vec{P}^{\odot}) \right) \\ & + \delta_L \left[\sin(2\varphi_{\gamma}) (I^S + \vec{\Lambda} \cdot \vec{P}^S) + \cos(2\varphi_{\gamma}) (I^C + \vec{\Lambda} \cdot \vec{P}^C) \right] \end{aligned} \right\}$$

- δ_{\odot}, δ_L : beam polarization ;
- $\vec{\Lambda}$: target polarization

$$\frac{d\sigma}{dx_i} = \sigma_0 \{ (1 + \Lambda_z \cdot \mathbf{P}_z) + \delta_{\odot} (I^{\odot} + \Lambda_z \cdot \mathbf{P}_z^{\odot}) \}$$

helicity difference
 beam-helicity
 beam-target

\mathbf{P}_z and I^{\odot} are odd functions of ϕ'

$$P_z = \frac{1}{\Lambda_z} \frac{[N(\rightarrow\Rightarrow) + N(\leftarrow\Rightarrow)] - [N(\rightarrow\Leftarrow) + N(\leftarrow\Leftarrow)]}{[N(\rightarrow\Rightarrow) + N(\leftarrow\Rightarrow)] - [N(\rightarrow\Leftarrow) + N(\leftarrow\Leftarrow)]}$$

$$I^{\odot} = \frac{1}{\delta_{\odot}} \frac{[N(\rightarrow\Rightarrow) + N(\rightarrow\Leftarrow)] - [N(\leftarrow\Rightarrow) + N(\leftarrow\Leftarrow)]}{[N(\rightarrow\Rightarrow) + N(\rightarrow\Leftarrow)] + [N(\leftarrow\Rightarrow) + N(\leftarrow\Leftarrow)]}$$

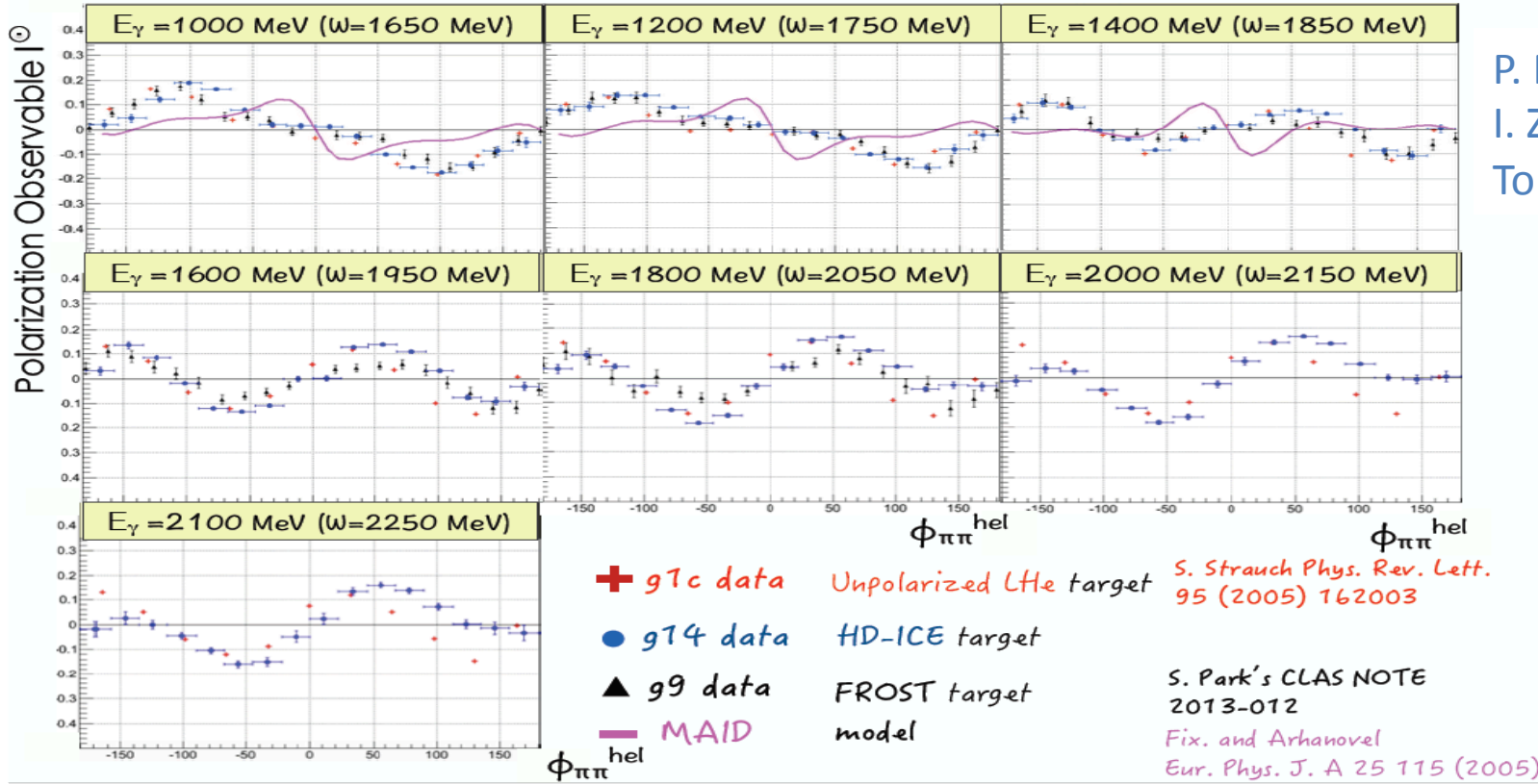
$$P_z^{\odot} = \frac{1}{\Lambda_z \delta_{\odot}} \frac{[N(\rightarrow\Rightarrow) + N(\leftarrow\Leftarrow)] - [N(\rightarrow\Leftarrow) + N(\leftarrow\Rightarrow)]}{[N(\rightarrow\Rightarrow) + N(\leftarrow\Leftarrow)] + [N(\rightarrow\Leftarrow) + N(\leftarrow\Rightarrow)]}$$

$I^{\odot} \quad \gamma p \rightarrow \pi^+ \pi^- p$ and $\gamma d \rightarrow \pi^+ \pi^- n(p)$

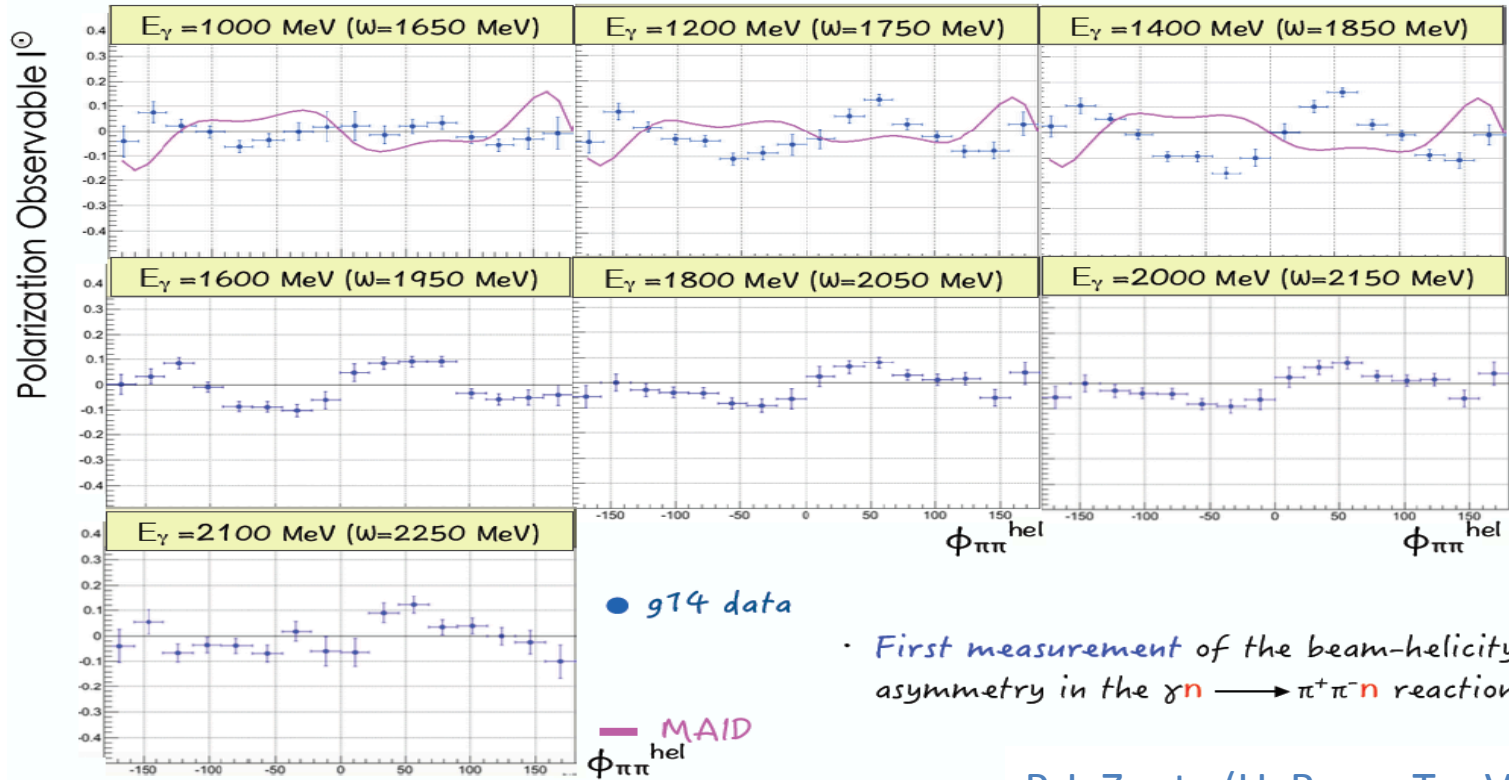


P. Peng (UVa),
I. Zonta (U. Roma
Tor Vergata)

- $P_{33}(1232)$
- $P_{11}(1440)$
- $D_{13}(1520)$
- $S_{11}(1535)$
- $S_{11}(1620)$
- $D_{15}(1675)$
- $F_{15}(1680)$
- $D_{33}(1700)$
- $P_{13}(1720)$



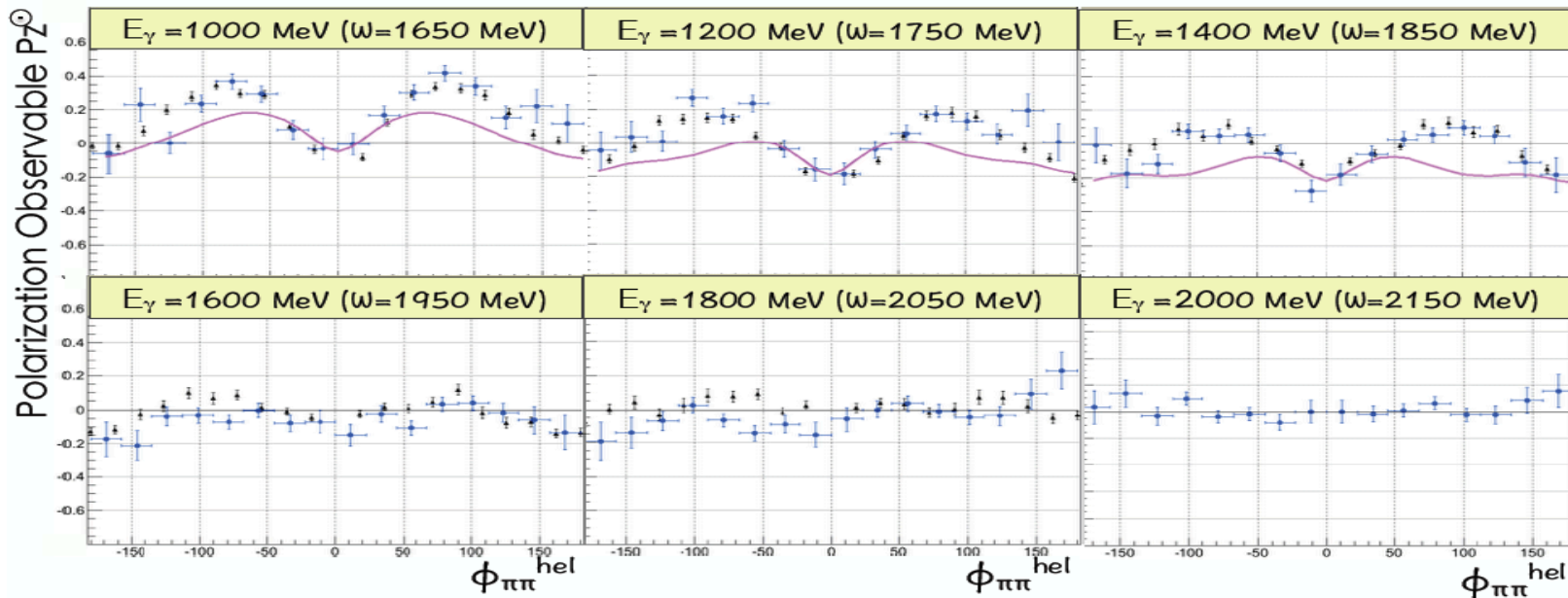
I^{\odot} for $\gamma d \rightarrow \pi^+ \pi^- n(p)$



• First measurement of the beam-helicity asymmetry in the $\gamma n \rightarrow \pi^+ \pi^- n$ reaction

P. I. Zonta (U. Roma Tor Vergata)

P_Z^\odot for $\gamma p \rightarrow \pi^+ \pi^- p$ and $\gamma d \rightarrow \pi^+ \pi^- p(n)$

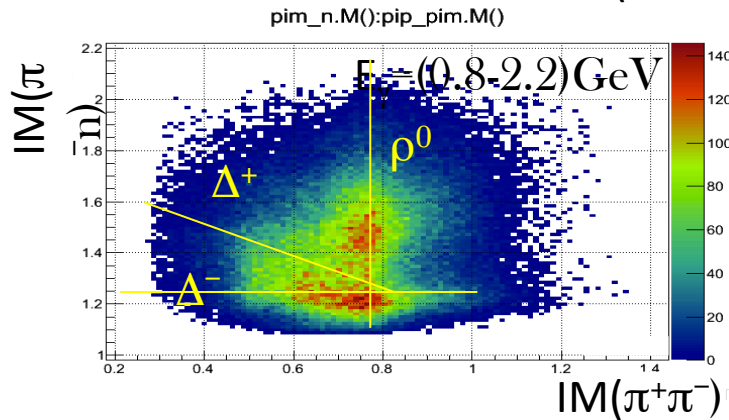
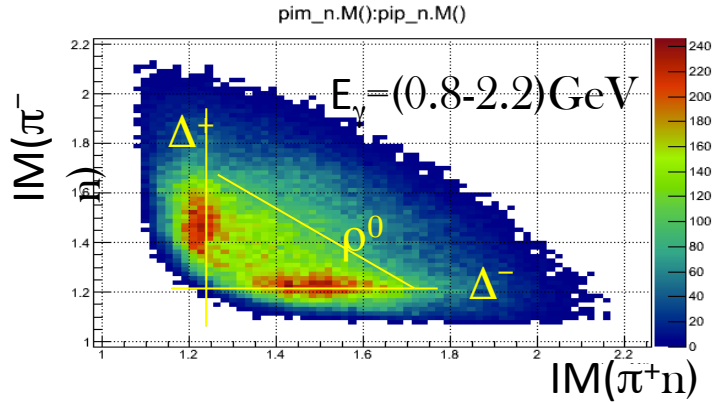


- g14 data HD-ICE target
- ▲ g9 data FROST target
- MAID model

P. I. Zonta (U. Roma Tor Vergata)

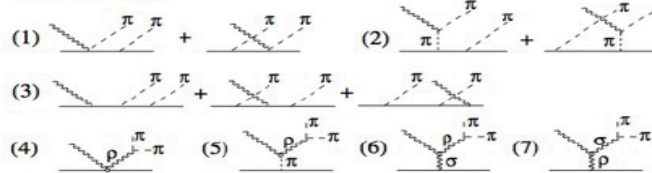
$\gamma p \rightarrow \rho p \rightarrow \pi^+ \pi^- p$ $\gamma d \rightarrow \rho n(p) \rightarrow \pi^+ \pi^- n(p)$

P. I. Zonta (U. Roma Tor Vergata)

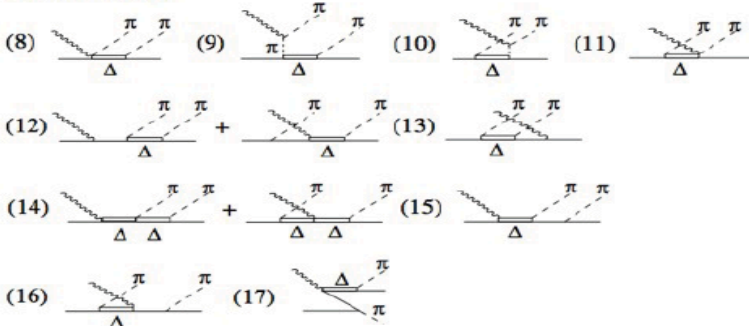


Diagrams for the reaction $\gamma N \rightarrow \pi\pi N$

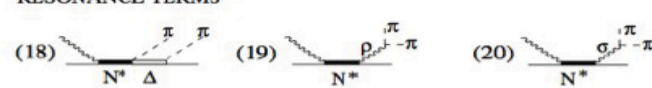
N-BORN TERMS



Δ -BORN TERMS



RESONANCE TERMS

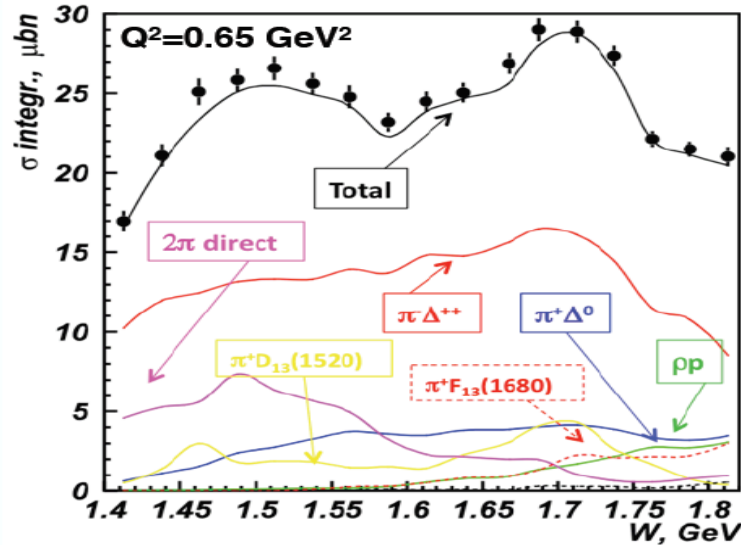
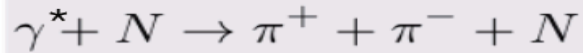


A. Fix and H. Arenhovel, Eur.Phys.J. A25 (2005) 115, nucl-th/0503042.

$\gamma p \rightarrow \rho p \rightarrow \pi^+ \pi^- p$



P. I. Zonta (U. Roma Tor Vergata)



it's the final states of
several possible reactions

disentangled for
electroproduction
by V. Mokeev

by V. Mokeev (JLab-Moscow model)

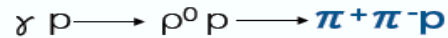
$\gamma p \rightarrow \rho p \rightarrow \pi^+ \pi^- p$



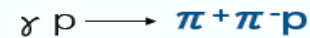
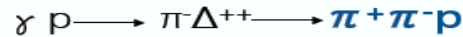
1) *SELECTION*: $IM(\pi^+ p) > 1.3 \text{ GeV}$ and $IM(\pi^- p) > 1.3 \text{ GeV}$

P. I. Zonta (U. Roma Tor Vergata)

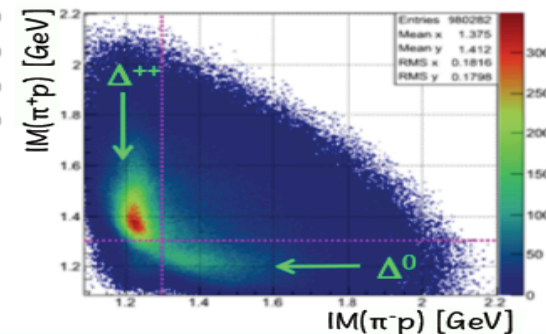
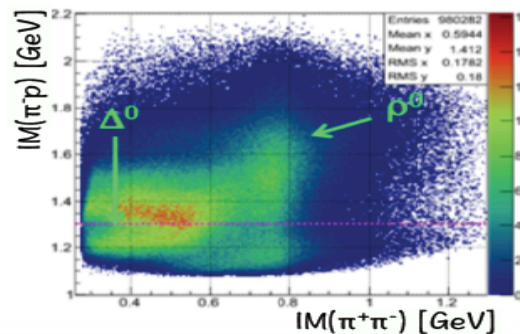
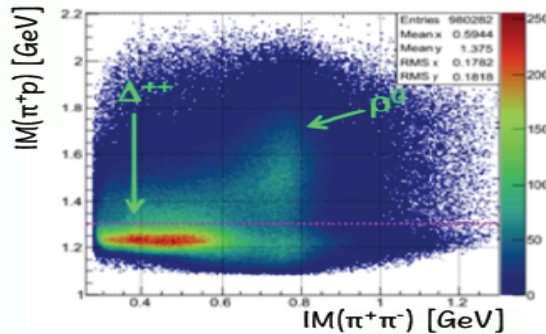
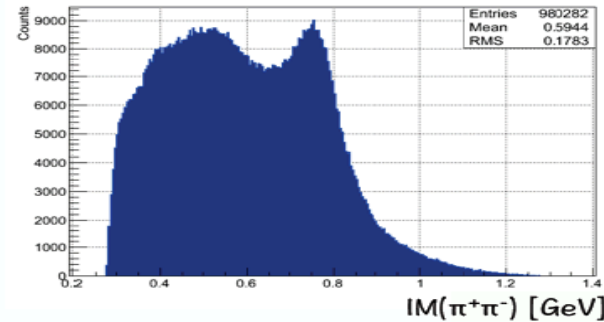
Goal \rightarrow disentangle the reaction:



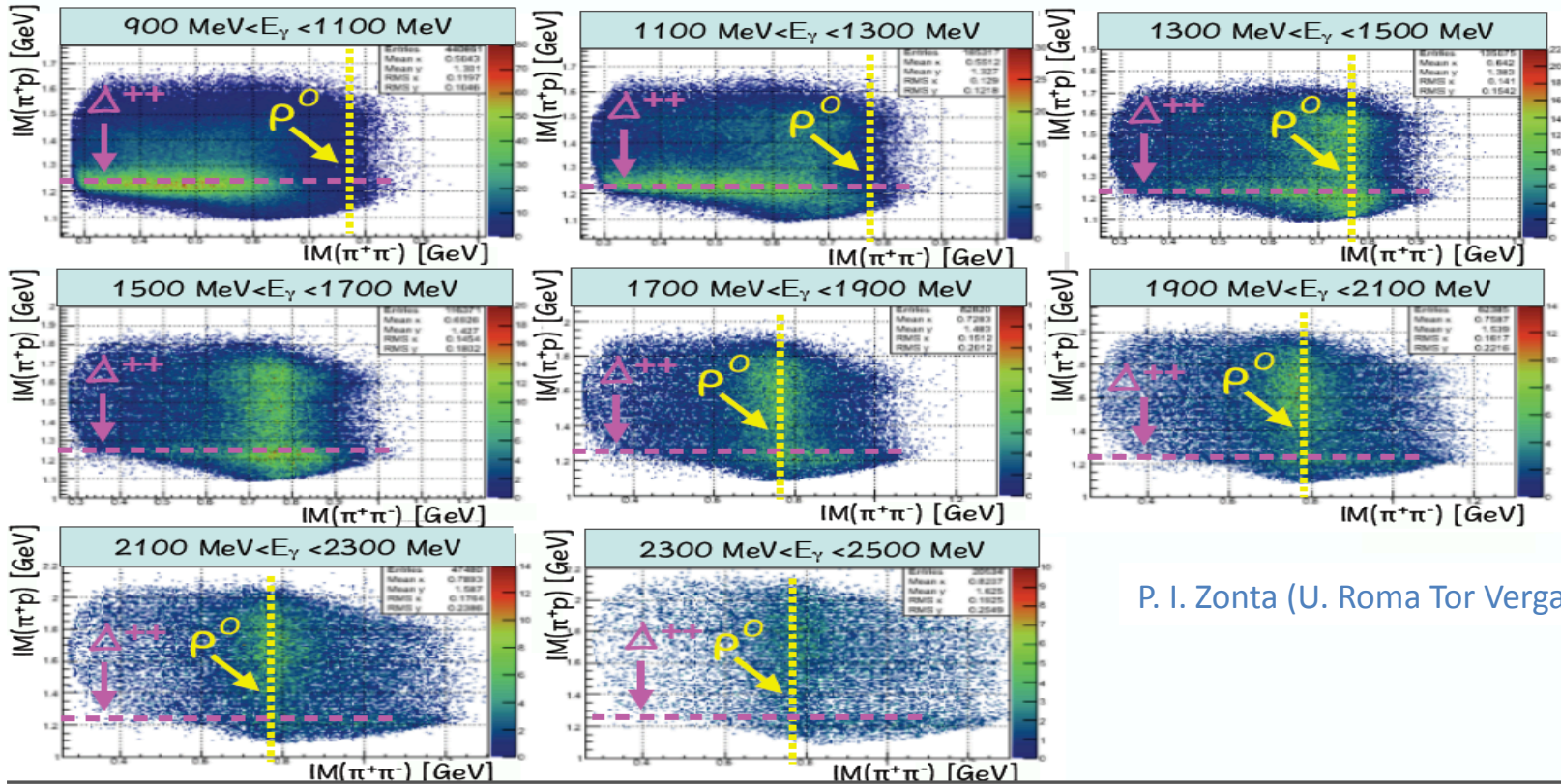
From the three concurrent reactions:



$IM(\pi^+ \pi^-)$ spectrum

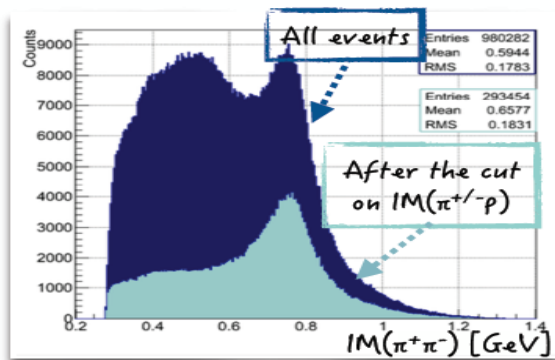


$\gamma p \rightarrow \rho p \rightarrow \pi^+ \pi^- p$

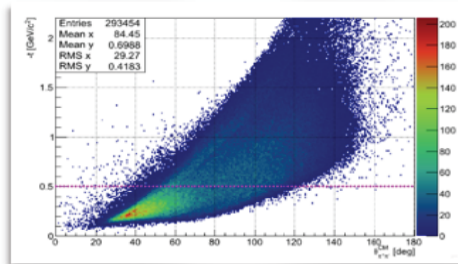


P. I. Zonta (U. Roma Tor Vergata)

$\gamma p \rightarrow \rho p \rightarrow \pi^+ \pi^- p$

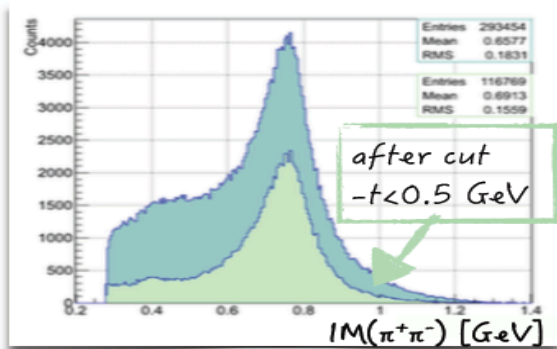


2) **SELECTION:** cut on $-t < 0.5$ GeV

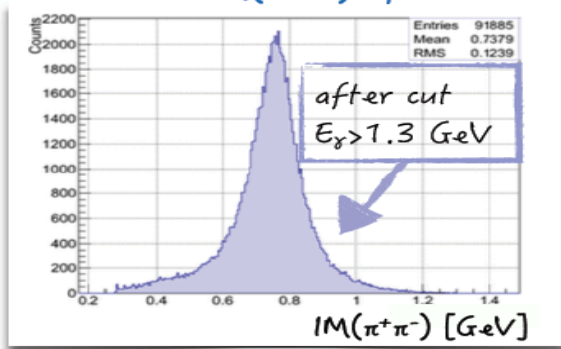


$-t$ vs. $\theta(\pi^+\pi^-)^{CM}$

3) **SELECTION:** cut on $E_\gamma > 1.3$ GeV



Final $IM(\pi^+\pi^-)$ spectrum

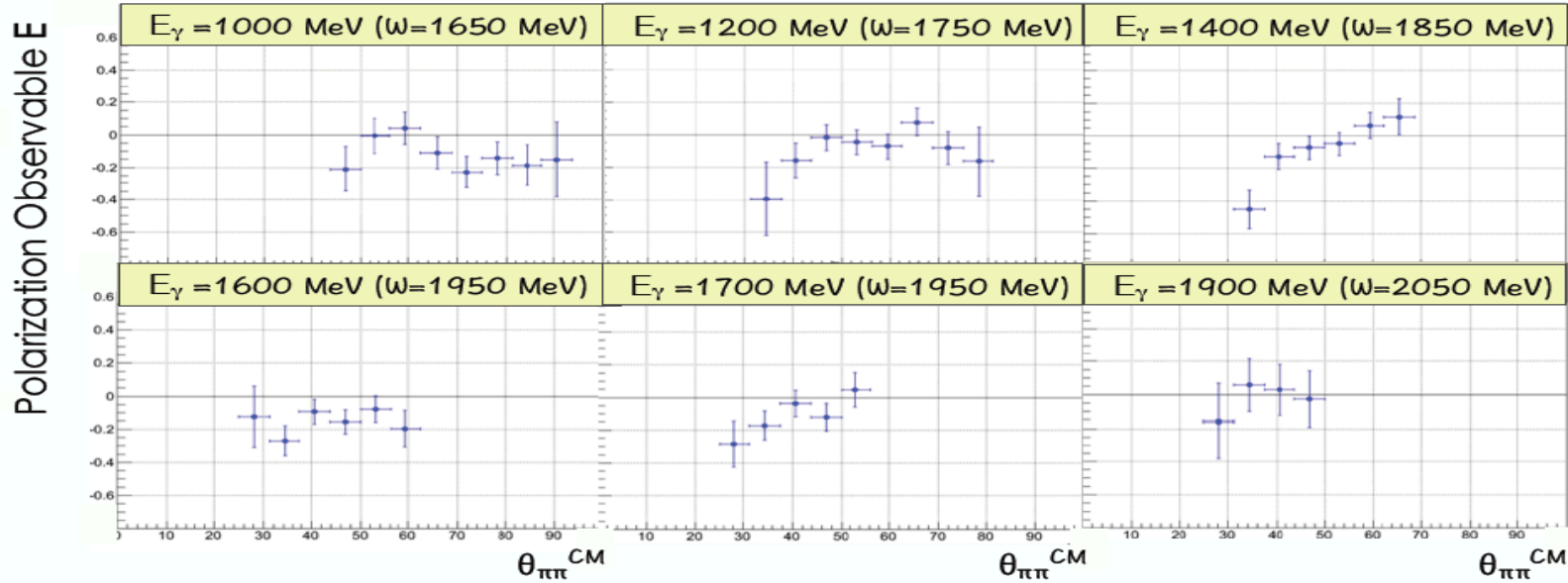


Events selection:

- $Im(p\pi^+) > 1.3$ GeV
- $Im(p\pi^-) > 1.3$ GeV
- $t < 0.5$ GeV
- $E_\gamma > 1.3$ GeV

P. I. Zonta (U. Roma Tor Vergata)

$\gamma p \rightarrow \rho p \rightarrow \pi^+ \pi^- p$



● *g14 data* *HD-ICE target*

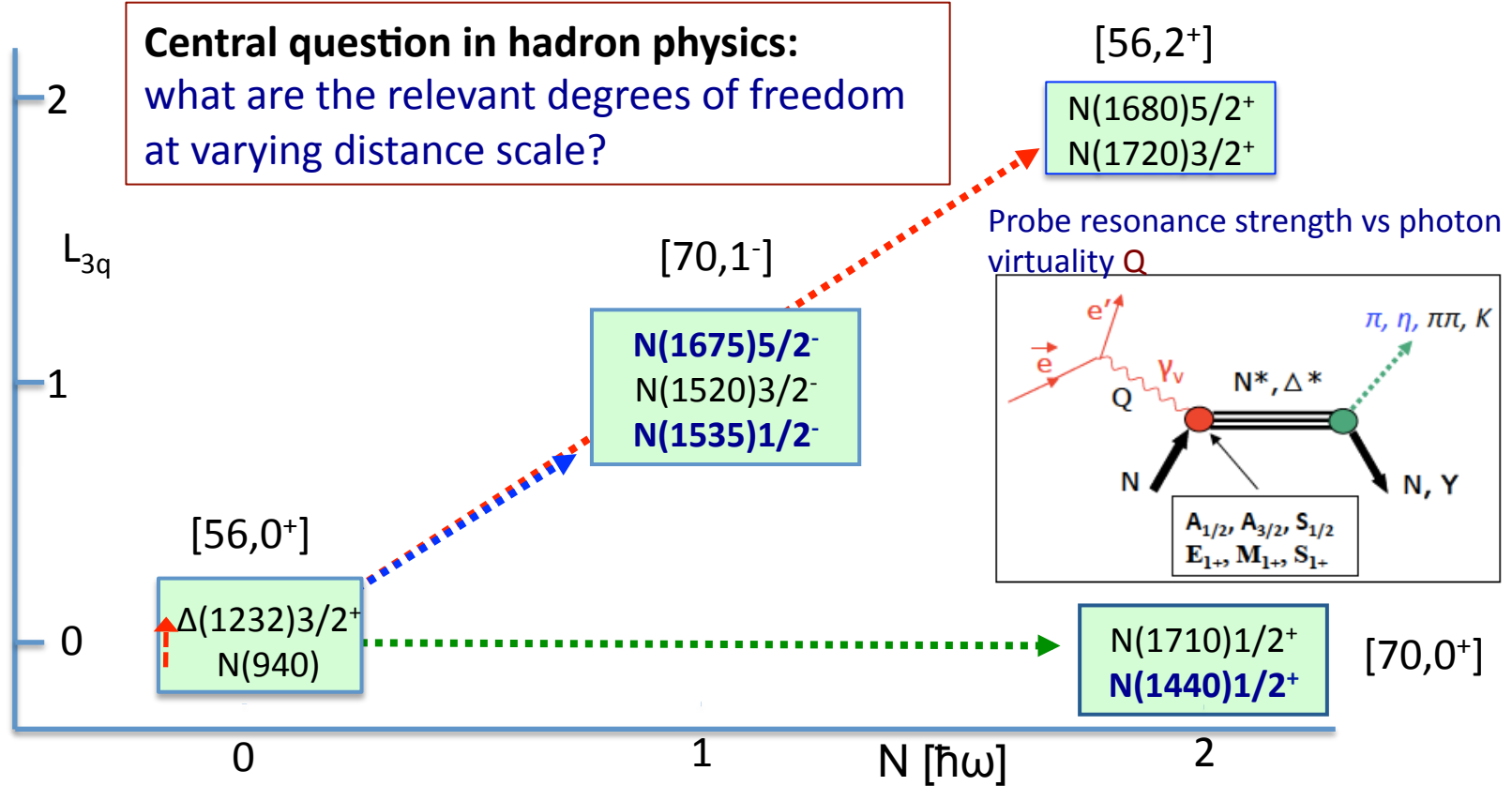
- *First measurement of the beam-target asymmetry*

Very preliminary

P. I. Zonta (U. Roma Tor Vergata)

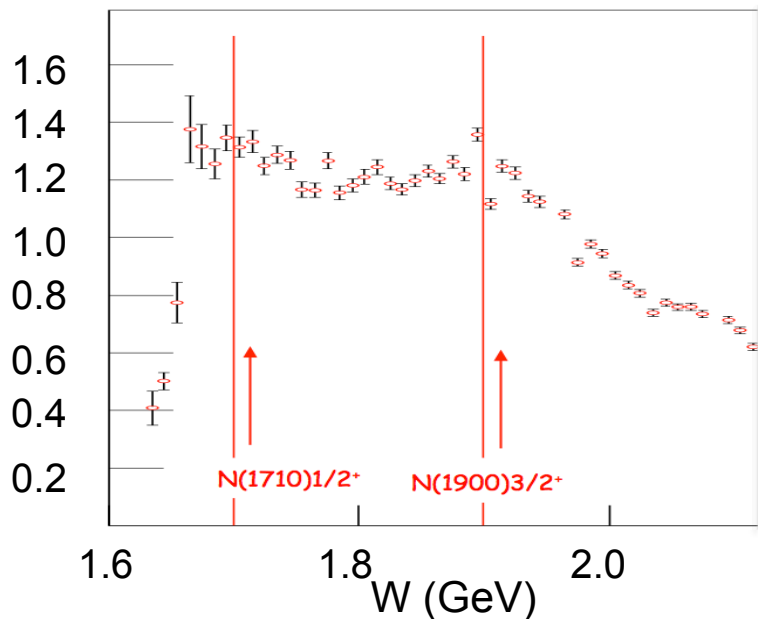
Electroexcitation of N^*/Δ resonances

Central question in hadron physics:
what are the relevant degrees of freedom
at varying distance scale?

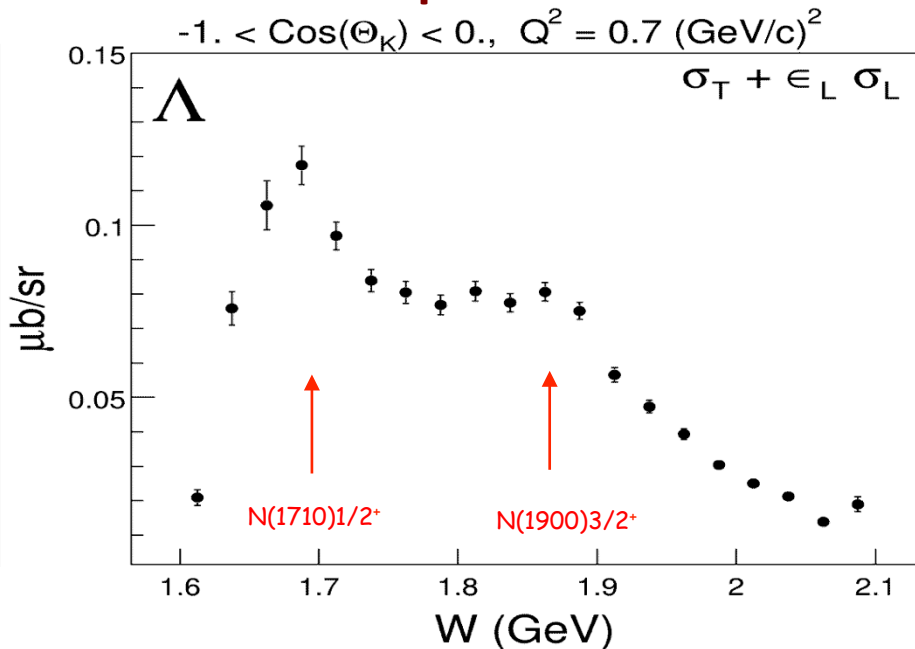


Studying Baryons in $\gamma^*p \rightarrow \Lambda/\Sigma$?

Photoproduction

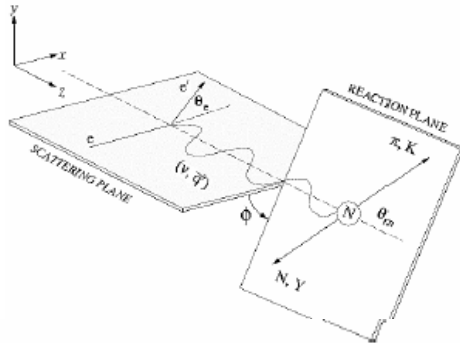


Electroproduction



Strangeness electroproduction is a fertile ground in studying $S=0$ baryon states with masses above 1.6 GeV.

Electroexcitation kinematics



$$\frac{d^4\sigma}{dQ^2 dW d\Omega_K} = \Gamma(Q^2, W) \times \frac{d\sigma}{d\Omega_K}(Q^2, W, \Theta_K, \varepsilon, \phi)$$

Virtual
photon
flux

Electroproduction
cross section

$$\frac{d\sigma}{d\Omega_K} = \underbrace{\sigma_T + \varepsilon_L \sigma_L + \varepsilon \sigma_{TT}}_{\sigma_u \text{ "Unseparated" (Transverse)}} \cos(2\phi) + \underbrace{\sqrt{2\varepsilon_L(\varepsilon+1)} \sigma_{LT}}_{\text{Transverse-longitudinal interference}} \cos(\phi) + h \sqrt{2\varepsilon_L(1-\varepsilon)} \underbrace{\sigma_{LT'}}_{\text{Helicity structure (Transverse-tra interference)}}$$

Transverse

Transverse-tra interference

Helicity structure

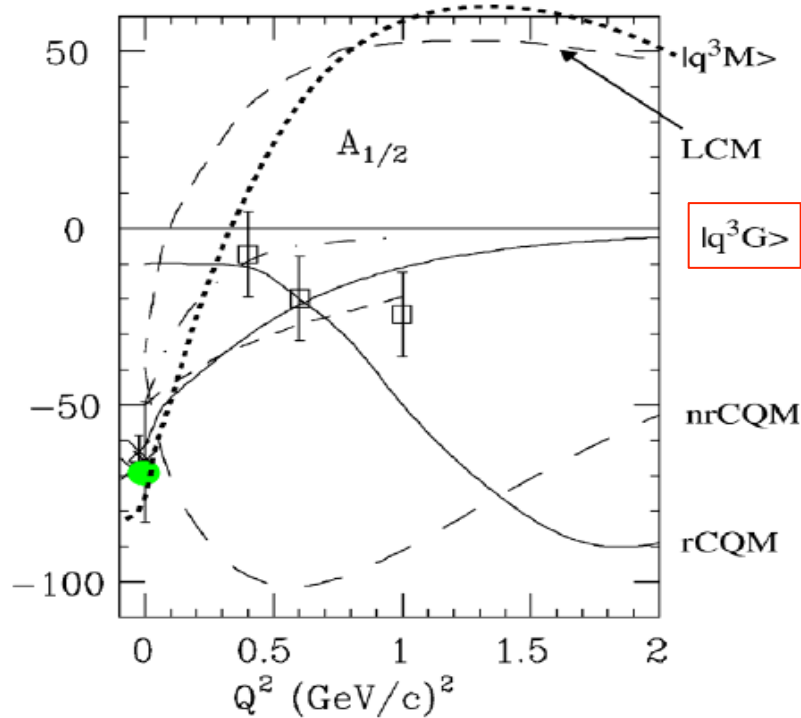
σ_u
"Unseparated"

Longitudinal (sensitive to $J=0^\pm$ exchange in t-channel: mesons, diquarks)

Transverse-longitudinal interference

Measured σ are decomposed using UIM or fixed-t DR to extract N^* & Δ helicity amplitudes.

Electrocouplings of the 'Roper' in 2002

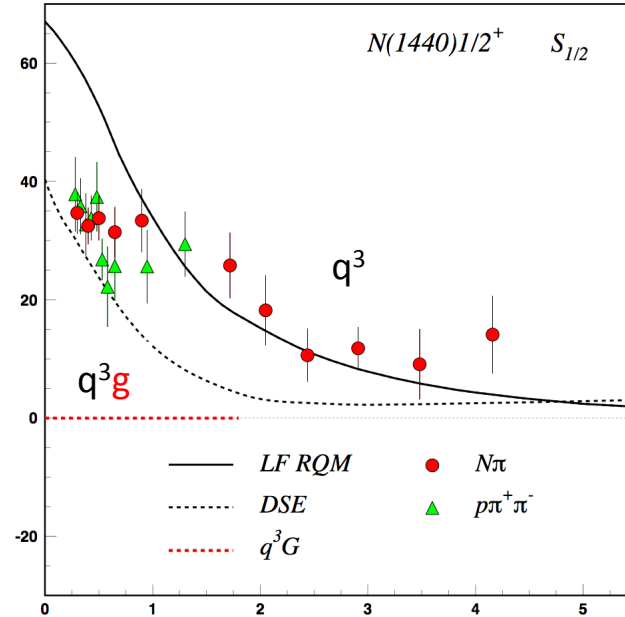
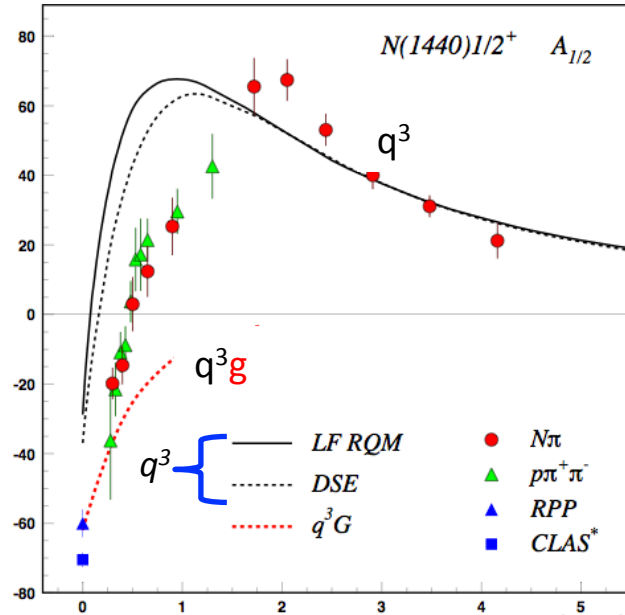


$N(1440)1/2^+$

In 2002 Roper amplitude $A_{1/2}$ measurements were more consistent with hybrid state but data were limited with large uncertainties.

Separating q^3g from q^3 states ?

CLAS results on electrocouplings clarified nature of the Roper: the structure is driven by the interplay of the core of three dressed quarks and the 1st radial excitation of the external meson-baryon cloud



Will CLAS12 data be able to identify gluonic contributions ?

For hybrid “Roper”, $A_{1/2}(Q^2)$ drops off faster with Q^2 and $S_{1/2}(Q^2) \sim 0$.

Hybrid Baryons: Baryons with Explicit Gluonic Degrees of Freedom

Hybrid hadrons with dominant gluonic contributions are predicted to exist by QCD.

Experimentally:

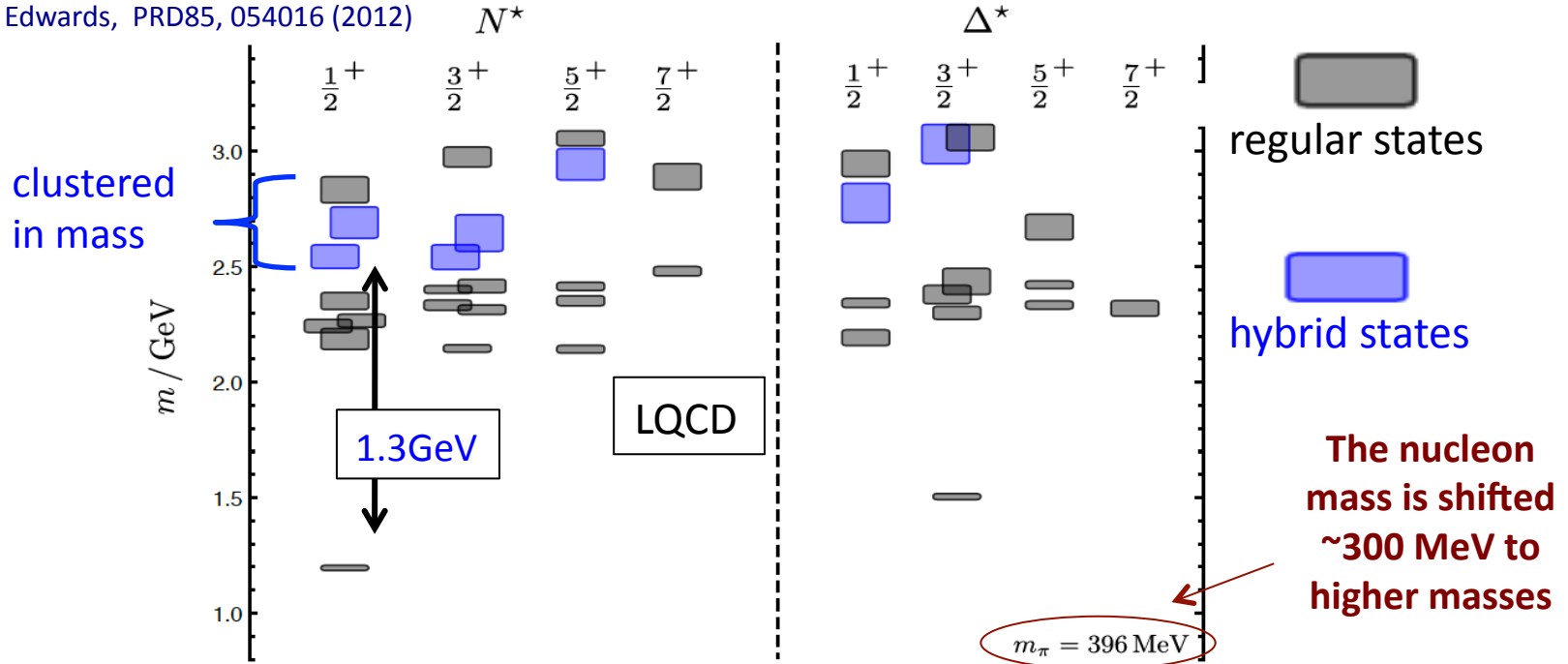
- **Hybrid mesons** $|qqg\rangle$ states may have exotic quantum numbers J^{PC} not available to pure $|qq\rangle$ states
GlueX, MesonEx, COMPASS, PANDA
- **Hybrid baryons** $|qqqg\rangle$ have the same quantum numbers J^P as $|qqq\rangle$ electroproduction with CLAS12 (Hall B).

Theoretical predictions:

- ✧ MIT bag model - T. Barnes and F. Close, Phys. Lett. 123B, 89 (1983).
- ✧ QCD Sum Rule - L. Kisslinger and Z. Li, Phys. Rev. D 51, R5986 (1995).
- ✧ Flux Tube model - S. Capstick and P. R. Page, Phys. Rev. C 66, 065204 (2002).
- ✧ LQCD - J.J. Dudek and R.G. Edwards, PRD85, 054016 (2012).

Hybrid Baryons in LQCD

J.J. Dudek and R.G. Edwards, PRD85, 054016 (2012)



Hybrid states have same J^P values as qqq baryons. How to identify them?

- Overpopulation of $N \frac{1}{2}^+$ and $N \frac{3}{2}^+$ states compared to QM projections.
- $A_{1/2}$ ($A_{3/2}$) and $S_{1/2}$ show different Q^2 evolution.

Hybrid Baryon Signatures

Based on available knowledge, the *signatures* for hybrid baryons consist of:

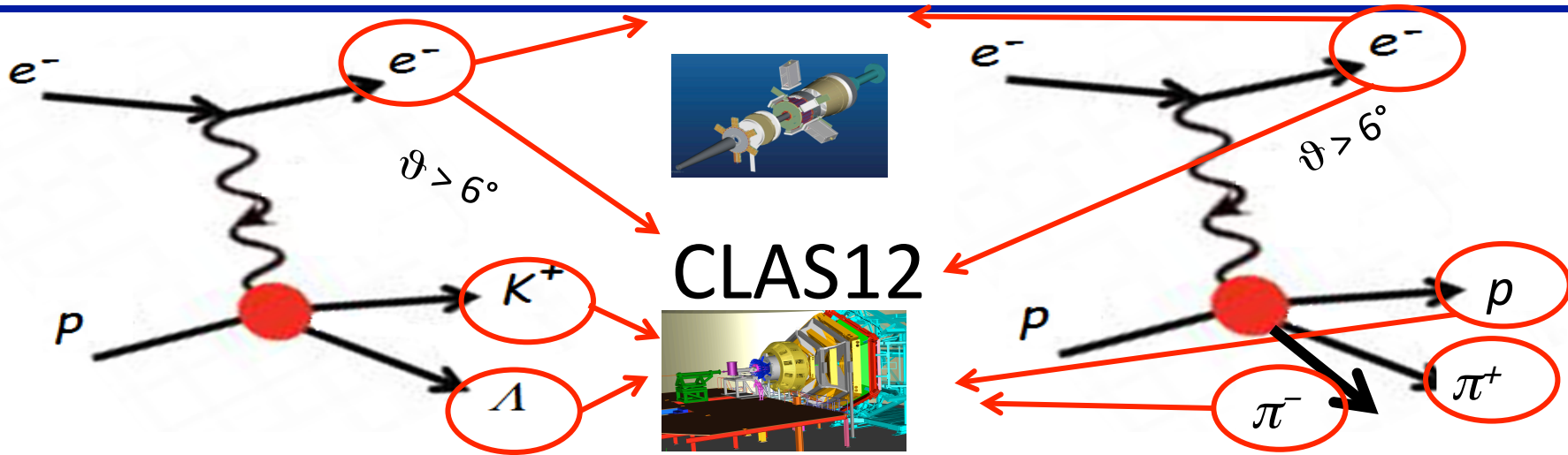
- **Extra resonances** with $J^P=1/2^+$ and $J^P=3/2^+$, with masses > 1.8 GeV and decays into $N\pi\pi$ or KY final states.
- A **drop** of the transverse helicity amplitudes $A_{1/2}(Q^2)$ and $A_{3/2}(Q^2)$ faster than for ordinary three quark states, because of extra glue-component in valence structure.
- A **suppressed** longitudinal amplitude $S_{1/2}(Q^2)$ in comparison with transverse electro-excitation amplitude ($J^P=1/2^+$).

We focused on:

$$e p \longrightarrow e p \pi^+ \pi^-$$

$$e p \longrightarrow e K^+ \Lambda, e K^+ \Sigma^0$$

The Experiment



Scattered electrons will be detected:

- in the Forward Tagger for angles from 2.5° to 4.5°
- in the Forward Detector of CLAS12 for scattering angles greater than about 6°

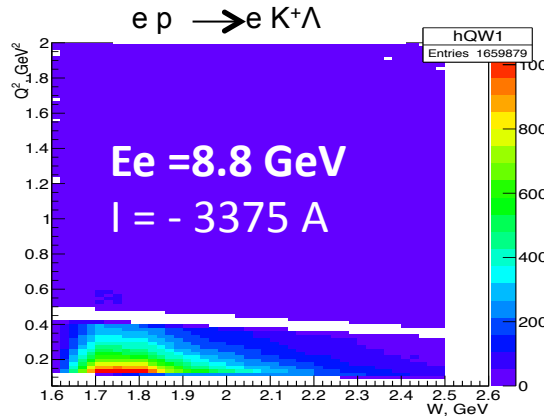
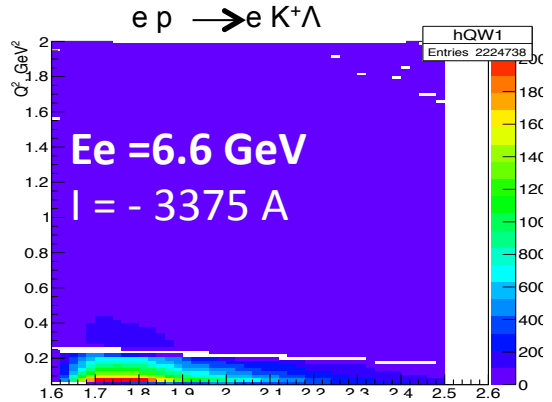
Charged hadrons will be measured in the full range from 6° to 130°

$W < 3 \text{ GeV}$ Q^2 range of interest: **0.05 - 2 GeV²**

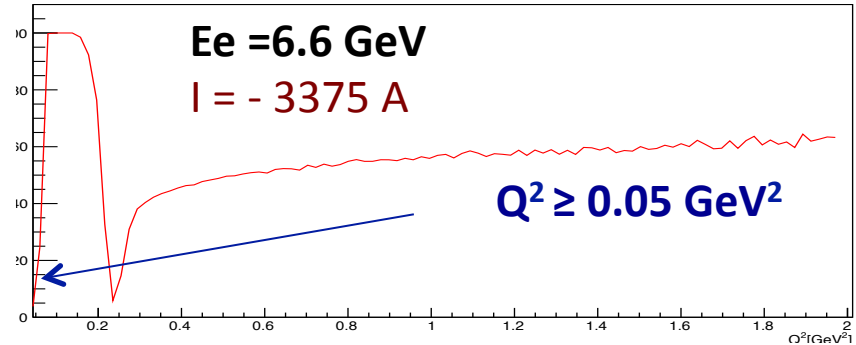
$$Q^2 = 4E_{\text{Beam}} E_{e'} \sin^2 \frac{\vartheta}{2} \Rightarrow \vartheta < 5^\circ$$

FT allows to probe the **crucial Q^2 range** where hybrid baryons may be identified due to their fast dropping $A_{1/2}(Q^2)$ amplitude and the suppression of the scalar $S_{1/2}(Q^2)$ amplitude.

Kinematical Coverage: Full Q^2 Range

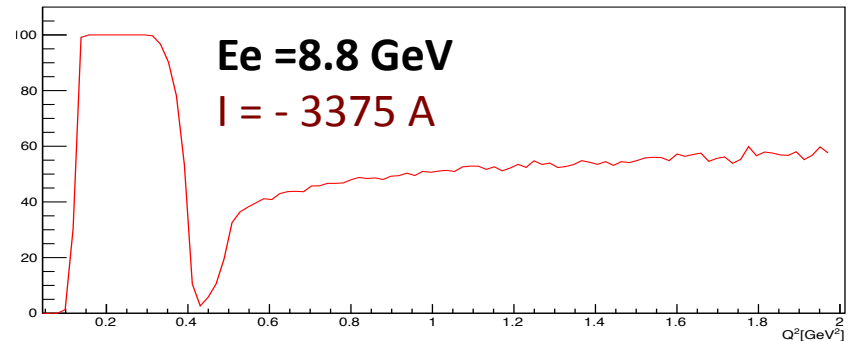


Single electron geometrical detection efficiency $E = 6.6 \text{ GeV}$



Q^2 as low as 0.05 GeV^2 may be reached

Single electron geometrical detection efficiency $E = 8.8 \text{ GeV}$



Quasi – Data Analysis

A hypothetical hybrid baryon contribution added at the amplitude level to the best presently available model RPR-2011:

$$M_R = 2.2 \text{ GeV} \quad \Gamma_R = 0.25 \text{ GeV} \quad J^P = 1/2^+ \quad (J^P = 3/2^+)$$

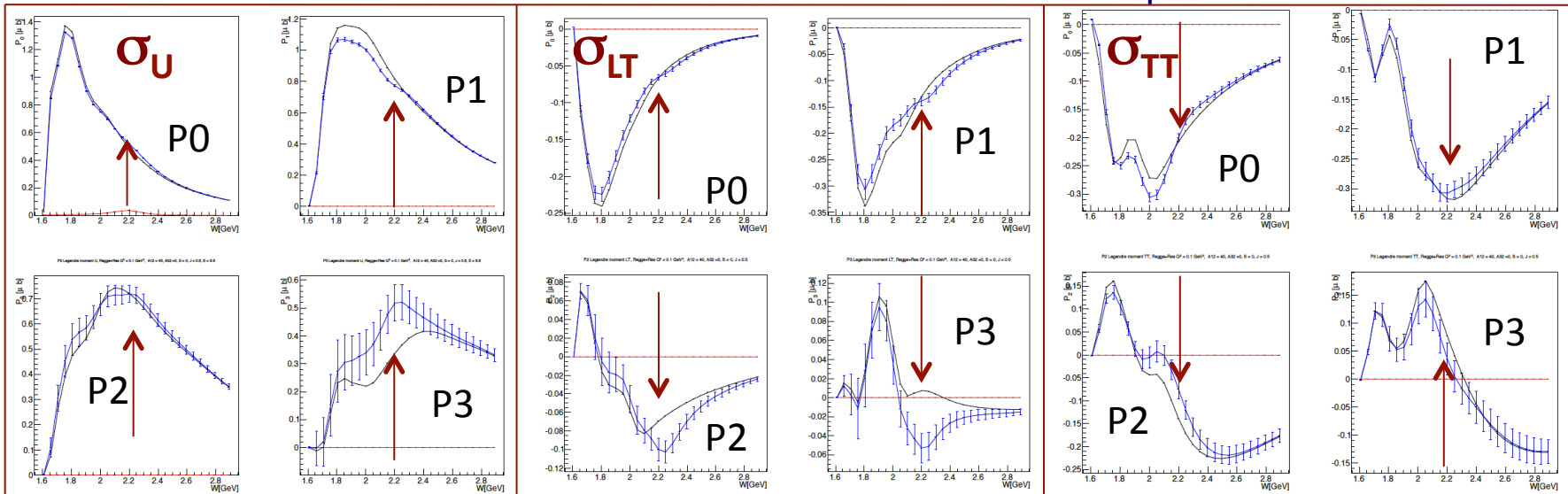
The reaction cross section has been calculated **with** and **without** the hybrid baryon resonance contribution to determine:

1. Minimum beam time needed to obtain statistical uncertainty for cross sections comparable with CLAS photoproduction data.
 - 100 days of beam time (50 days at 6.6 GeV & 50 days at 8.8 GeV)
2. The Legendre moments of the unseparated and polarization interference components of the cross section.
 - Search for distinctive structures due to the added resonance.
3. The statistical sensitivity to hybrid baryons electrocouplings.
 - Minimum electrocoupling values with 100 days of beam time.
4. The capability of extracting the added resonance parameters from expected data.
 - Blind analysis of quasi-data.

Extraction of Legendre Moments

$e p \rightarrow e K^+ \Lambda$ First Legendre Moments

Black curves RPR 2011 model
Blue points RPR 2011 + Resonance



- $J = \frac{1}{2}$ Regge + Res. $Q^2 = 1 \text{ GeV}^2$ $M_{\text{res}} = 2.2 \text{ GeV}$ $A_{1/2} = 0.04 \text{ GeV}^{-1/2}$ $S_{1/2} = 0$
Significant structures appear in most of the Legendre moments at the value of $W = 2.2 \text{ GeV}$, corresponding to the mass of the added hybrid baryon

Statistical Sensitivity of Resonance Electrocouplings

$e p \rightarrow e K^+ Y$

Regge + Resonance (RPR-2011) Gent model

Fixing the resonance parameters: $M_{\text{res}} = 2.2 \text{ GeV}$, $\Gamma_{\text{res}} = 0.25 \text{ GeV}$, $S_{1/2} = 0$

and varying $A_{1/2, 3/2} \longrightarrow$ **Minimum values for hybrid baryons electrocouplings**

$$\chi^2 / d.p. = \frac{1}{N_{d.p.}} \sum_{W, \cos\theta^* \phi} \frac{(d\sigma_{\text{mod}} - d\sigma_{\text{mod+res}})^2}{(d\sigma_{\text{mod}} + d\sigma_{\text{mod+res}}) / N_{ev}}$$

To be compared with **N(1440)1/2⁺**

$Q^2 \text{ (GeV}^2\text{)}$	$J_R = 1/2$		$J_R = 3/2$		
	$A_{1/2}$	$S_{1/2}$	$A_{1/2}$	$A_{3/2}$	$S_{1/2}$
$\times 10^{-3} \text{ (GeV}^{-1/2}\text{)}$					
0.1	9.5	9.5	13	8.5	8.5
0.5	14	16	15	15	10
1.0	13	19	14	14	7.5

$Q^2 \text{ (GeV}^2\text{)}$	0.	0.65	1.3
$A_{1/3} \times 10^{-3} \text{ (GeV}^{-1/2}\text{)}$	-70	10	30

Blind Extraction: $J^P=1/2^+ + J^P=3/2^+$

Two hybrid baryon resonances with $J^P = 1/2^+$ and $J^P = 3/2^+$ were inserted in the ep \rightarrow e $K^+\Lambda$ Gent RPR2011 reaction amplitude and quasi-data were generated $\longrightarrow d\sigma_{q.d.}$

A blind analysis has been then attempted trying to extract the resonances J^P spin-parities and

7 unknown parameters: $M_{res}^1 \Gamma_{res}^1 A_{1/2}^1$
 $M_{res}^2 \Gamma_{res}^2 A_{1/2}^2 A_{3/2}^2$

Searching the minimum of the quantity:

$$\chi^2 / d.p. = \frac{1}{N_{d.p.}} \sum_{W, \cos\theta^*, \phi} \frac{(d\sigma_{th} - d\sigma_{q.d.})^2}{(d\sigma_{q.d.}) / N_{ev}}$$

$d\sigma_{th}$ were calculated using the **Gent RPR2011** amplitudes including two resonances $J^P = 1/2^+$ and $J^P = 3/2^+$, whose parameters values were scanned in the range:

$$2.0 < W < 2.5 \text{ GeV} \quad -0.05 < A_{1/2} < +0.05 \text{ GeV}^{-1/2}$$

$$0.1 < \Gamma < 0.4 \text{ GeV} \quad -0.05 < A_{3/2} < +0.05 \text{ GeV}^{-1/2}$$

at a fixed $Q^2 = 0.5 \text{ GeV}^2$

$$S_{1/2} = 0$$

Blind Extraction: $J^P=1/2^+$ + $J^P=3/2^+$

Two hybrid baryon resonances with $J^P = 1/2^+$ and $J^P = 3/2^+$ were inserted in the $ep \rightarrow e K^+ \Lambda$ Gent RPR2011 reaction amplitude and **quasi-data** were generated $\longrightarrow d\sigma_{q.d.}$

A blind analysis has been then attempted trying to extract the resonances J^P spin-parities and

7 unknown parameters: M_{res}^1 Γ_{res}^1 $A_{1/2}^1$
 M_{res}^2 Γ_{res}^2 $A_{1/2}^2$ $A_{3/2}^2$

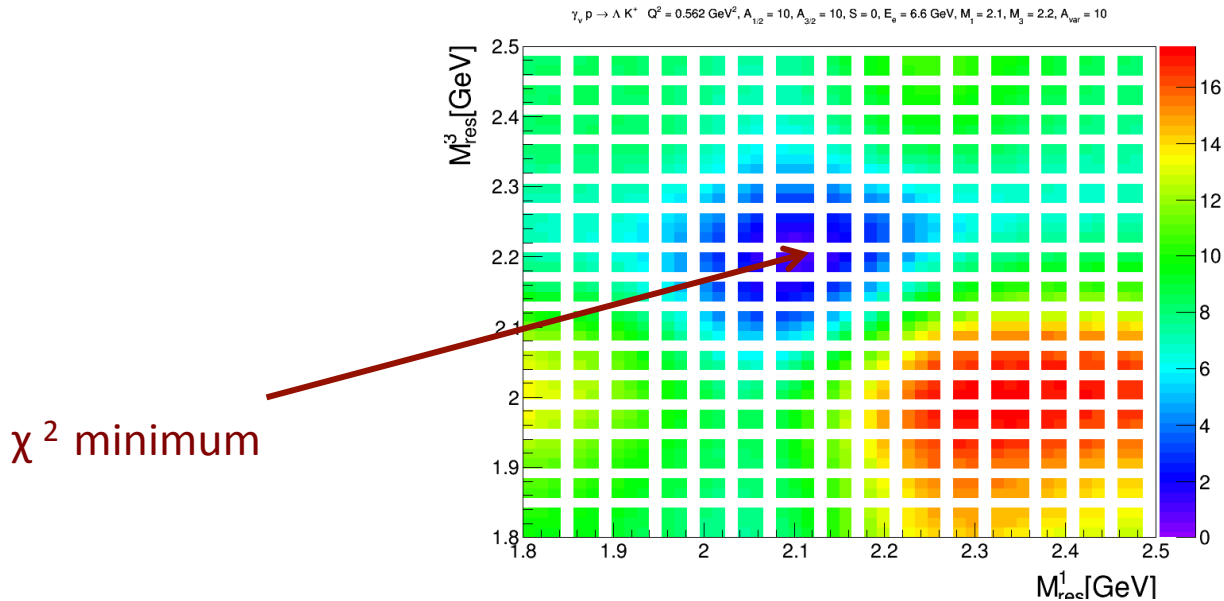
Iterative procedure:

- The algorithm calculates the χ^2 value over a 7-dim parameters coarse grid, covering the full range
- The combination of parameters corresponding to the minimum χ^2 value is found
- χ^2 value is calculated over a finer 7-dim parameters grid, around the minimum
- The procedure is repeated three times.

Blind Extraction: $J^P=1/2^+ + J^P=3/2^+$

Two hybrid baryon resonances with $J^P = 1/2^+$ and $J^P = 3/2^+$ were inserted in the $ep \rightarrow e K^+ \Lambda$ Gent RPR2011 reaction amplitude and **quasi-data** were generated $\longrightarrow d\sigma_{q.d.}$

Typical 3-dim map of χ^2 as a function of the two resonance masses, evolving in time for increasing $A_{1/2}$ ($A_{3/2}$) strength.



Blind Extraction: $J^P=1/2^+ + J^P=3/2^+$

Two hybrid baryon resonances with $J^P = 1/2^+$ and $J^P = 3/2^+$ were inserted in the $ep \rightarrow e K^+ \Lambda$ Gent RPR2011 reaction amplitude and **quasi-data** were generated $\longrightarrow d\sigma_{q.d.}$

A blind analysis has been then attempted trying to extract the resonances J^P spin-parities and
7 unknown parameters:

$$M_{res}^1 \quad \Gamma_{res}^1 \quad A_{1/2}^1 \\ M_{res}^2 \quad \Gamma_{res}^2 \quad A_{1/2}^2 \quad A_{3/2}^2$$

Hybrid Baryons parameters are well reconstructed.

Blind Resonance Parameters	Extracted Resonance Parameters
$M_{res}^1 = 2.30$ GeV	$M_{res}^1 = 2.32$ GeV
$\Gamma_{res}^1 = 0.30$ GeV	$\Gamma_{res}^1 = 0.30$ GeV
$A_{1/2}^1 = 0.020$ GeV ^{-1/2}	$A_{1/2}^1 = 0.019$ GeV ^{-1/2}
$M_{res}^2 = 2.45$ GeV	$M_{res}^2 = 2.45$ GeV
$\Gamma_{res}^2 = 0.35$ GeV	$\Gamma_{res}^2 = 0.31$ GeV
$A_{1/2}^2 = -0.015$ GeV ^{-1/2}	$A_{1/2}^2 = -0.014$ GeV ^{-1/2}
$A_{3/2}^2 = 0.04$ GeV ^{-1/2}	$A_{3/2}^2 = 0.038$ GeV ^{-1/2}

Baryon Spectroscopy Status Today

- Major progress made in the last ~ 5 years in the search for N^* and Δ states. All states can be accommodated in CQM and LQCD schemes.
 - Non-dynamical di-quark models are ruled out.
- Knowledge of Q^2 -dependence of electrocouplings is absolutely necessary to understand the nature (the internal structure) of the excited states.
 - Roper IS the first radial excitation of the q^3 core, obscured at large distances by meson-cloud effects.
- Leading electrocoupling amplitudes of prominent low-mass states (e.g. $N(1535)1/2^-$) is well modeled by DSE/QCD, LC SR and LF RQM for $Q^2 > 2$ GeV.
- Search for hybrid baryons with explicit gluonic degrees of freedom would be possible investigating the low Q^2 evolution of high-mass resonance (2-3 GeV) electrocouplings:
 - Looking for suppressed $A^{1/2}$, $A^{3/2}$, $S^{1/2}$ at low Q^2 .